

ERASMUS UNIVERSITY ROTTERDAM

Erasmus School of Economics

Master Thesis Econometrics and Management Science

Testing for structural breaks in the KNW model

Name student: Rijk van Oostenbrugge

Student ID number: 432778

Supervisor: dr. J.W.N. Reuvers

Second assessor: dr. W. Wang

Date: April 28, 2022

The content of this thesis is the sole responsibility of the author and does not reflect the view of the supervisor, second assessor, Erasmus School of Economics or Erasmus University.

Abstract

In this paper we test for structural breaks in the parameters of the KNW model using a SupLR test, and we compare the fit of the current two-factor KNW model with a three-factor KNW model. We find that there is evidence of a structural break in the sample between January 1999 and May 2021, which occurs in October 2008 in three of the four tested model specifications, coinciding with the ECB's introduction of the fixed rate full allotment policy. The remaining model specification finds a break in September 2008, which can be seen as one of the critical months in the financial crisis, with e.g., the bankruptcy of Lehman Brothers. Furthermore, we find that the three-factor specification of the KNW model shows a better fit, when using the AIC and BIC. When using the sample after October 2008, we find that this result is not affected by the structural break in 2008. Lastly, we observe the implications of scenarios generated from the estimated parameters and find that zero coupon bond rates are lower after the break in all model specifications, when compared to their full sample scenarios.

1 Introduction

Dutch pension funds are required by law to periodically perform an achievability test (Haalbaarheidstoets in Dutch) such that the funds can assess whether their current investment policies align with their ambitions in their pension returns over the full horizon in which participants are allowed to receive their returns. The introduction of this test has led pension funds to make their risk attitude concrete (Lever, 2019), making this beneficial for both the pension fund and the fund participant. To do this test, the Dutch Central bank (DNB) quarterly generates 10000 scenarios of 60 years ahead for term structures, stock returns, and price inflation. These values are generated using an adaptation of the KNW model, which was introduced by Kojien et al. (2010). In this paper we research whether the parameters of this model are subject to structural breaks and whether the addition of a third factor would improve model fit.

The KNW model is a Gaussian affine model extending Brennan and Xia (2002) to include time-varying bond risk premia. Brennan and Xia (2002) extend the two-factor affine term structure model to include the stock price. Affine term structure models (ATSMs) have a rich existing literature behind them, starting at Vasicek (1977), who devised a one factor term structure model, using the short rate as factor. This is followed by Cox et al. (1985), allowing for a varying volatility, which depends on the value of the factor. Then Duffie and Kan (1996) and Dai and Singleton (2000) generalized the affine term structure model to allow for multidimensional factors.

The literature on the KNW model has been evolving steadily after its conception, starting with Draper (2014), which shows the derivation of the discretized KNW model and adds calibration to the model. Muns (2015) continues in this line by refining the calibration methods from Draper (2014) and derives closed-form expressions for the term structure, long-term expectations, and covariances. Bouwman and Lord (2016) extend the scope of the KNW model by deriving closed-form formulas for interest rate swaps, swaptions, inflation-linked swaps, and equity options in the context of the KNW model. Pelsser (2019) adds to the literature of the KNW model by rewriting the model into the form of a standard Kalman Filter, which allows for the construction of confidence intervals around the parameters. We find significant structural breaks in September and October of 2008, depending on model specification. Also, we find that the three-factor model shows a better fit, using the AIC and BIC, even when we only estimate the model after the break.

This paper finds academic relevance in adding to the literature of estimating the KNW model, and of detecting structural breaks in the Kalman Filter and term structure models.

Social relevance is found in testing and offering an alternative approach to calculate the parameters of the KNW model, which indirectly can lead to alternatives in the scenarios of the achievability test, which could potentially affect pension investment allocations. For example, since January of 2021 DNB has adjusted the parameters manually to ensure that the longer

term bond rates did not seem realistic anymore, as too high rates were found to be simulated¹. We explore whether a structural break would have an effect on this.

In Section 2 of the paper we will put the problem in theoretical perspective, after which we describe the data used in this paper in Section 3. Sections 4 and 5 will describe the methodology and the extensions of the paper, followed by Section 6, which covers the found results. We conclude the paper with the discussion in Section 7.

¹<https://www.dnb.nl/voor-de-sector/open-boek-toezicht-sectoren/pensioenfondsen/haalbaarheidstoets/uitvoering-en-normen/scenarioset-haalbaarheidstoets-pensioenfondsen/>

2 Theoretical Framework

In this section we treat the theoretical framework of the problem. First we discuss structural changes in zero coupon bond rates, where we find that monetary policy changes might lead to these structural changes. Therefore, we continue with a summary of the non-standard measures that the ECB have taken. Then we discuss how to detect structural breaks and conclude with a short history of the three-factor affine term structure models and how it links to the KNW model.

2.1 Structural changes in the term structure

Changes in the term structure and its causes have been studied widely using different techniques. Here we show a few cases. Hansen (2003) developed a statistical model to detect structural changes in vector error correction models (VECM) and applied this technique to monthly U.S. zero coupon bond yields from 1970 to 1995, with maturities varying from 1 to 84 months. This method provided statistical evidence of structural changes in September of 1972 and in October of 1982, which coincides with policy changes of the Federal Reserve.

Marçal and Pereira (2014) applied the methodology of Hansen (2003) to Brazilian zero coupon bonds, with maturity up to 3 years, between 1996 and 2011. The authors find a structural break in 2003, where risk premiums for these bonds decreased sharply. However, according to the authors this did not point to any policy changes coinciding with the break.

Andreasen et al. (2019) find Chow statistics exceeding the 95% critical value in the US bond yields from 1990 to 2018, using a Gaussian shadow rate models. The peaks of the Chow statistics differ for different bond maturities: For 3-, 5-, 7- and 10-year maturities this peaked in respectively 2003, 2008, 2009, and 2010. The peak in 2003 could be explained by recovery after the recession in the early 2000s, while the other peaks could be explained by the aftermath of the financial crisis of 2007. Furthermore, the authors find that the time-series dynamics of the pricing factors change once bond rates are near the Zero Lower Bound (ZLB). After the crisis of 2007, they also find that when the short rate is further from the ZLB, the bond risk premiums will behave as before the break in the financial crisis.

Lemke and Vladu (2016) critique the use of ATSMs in the cases that the yield curve nears the Zero Lower Bound, since the rates in ATSMs are able to become very negative, due to the Gaussian nature of the model. Furthermore, the authors find in the cases that when short rates are reaching the ZLB, these short rates will stick to the ZLB for a while, showing very low volatility. Therefore, the authors propose to use a shadow rate term structure model (SRTSM), which does not allow the short term rate to fall below the ZLB. Lastly, in their data set from 1999 to June 2015, the authors detect a shift in the effective lower bound in August 2014, where the lower bound shifts from 1 basis point to -11 basis points, which is attributed to an unexpected ECB rate cut.

2.2 Non-standard measures in monetary policy by the ECB

We see in the literature above that changes in term structure may be affected by changes in monetary policy. Hence, we summarize the non-standard measures that ECB has taken in the aftermath of the financial crisis of 2007 (European Central Bank, 2021).

The first measure was taken in October 2008 to ensure the liquidity of banks and the continuity of financial markets, as lack of liquidity in interbank markets had occurred. To prevent market failure, the ECB provided unlimited credit to banks at a fixed interest rate against adequate collateral and financial soundness of the bank (fixed full-rate allotment). Additionally, the range of eligible assets which could be used as collateral for the fixed full-rate allotment had been expanded, when compared to other refinancing operations.

This was followed by a phase in which the ECB faced the challenge of a sovereign debt crisis, which the ECB tried to mitigate this by addressing the malfunctioning of markets and the differences in financing conditions of households and businesses between different euro area countries. In May 2010, the ECB purchased debt securities. This was followed by the Very Long Term Refinancing Operations in December 2011. The nonstandard measures in this phase were concluded by the Outright Monetary Transactions in September 2012.

In the third and final phase in the wake of the financial crisis of 2007, the ECB had to mitigate the risks of a credit crunch and deflation. This was done by taking multiple nonstandard measures. The ECB started to apply forward guidance in July 2013, which entails that the ECB communicates the evolution of its policy and what events would trigger changes in policy stances. In June 2014, the interest rates were lowered to negative levels. This fell together with the introduction of Targeted Longer-Term Refinancing Operations (TLTROs), which provided long-term financing to credit institutions. Three series of TLTROs were launched, the first being in June 2014, the second in March 2016, and the third in March 2019. These measures were followed by the Asset Purchase Programmes between October 2014 and December 2018, which were introduced with the intention to lower the interest rate term structure and to aid price stability.

2.3 Structural breaks

The literature regarding structural breaks in time series is quite extensive and can be split in two parts: Firstly, the testing for the existence of a structural break and secondly, the determining of the amount of breaks in a time series. We treat the literature regarding the finding of a single structural break in Section 5.1 together with its methodology. In the determining of the amount of breaks there are two main approaches: The joint (simultaneous) approach in which all breaks are estimated at the same time, and the sequential approach in which breaks are estimated one by one. Bai and Perron (2003) introduced an efficient algorithm which computes the amount of breaks and its break points in linear models using a joint approach. This paper has been crucial due to the exponential scaling of computer time in the number of breaks that are tested for, making this approach feasible for linear models. The sequential approach has been introduced by

both Bai and Perron (1998) and Chong (1995). In the KNW model, we would use the sequential approach, due to the non-linearity of the problem. Non-linear problems, to our knowledge, do not yet have an efficient algorithm similar to Bai and Perron (2003) for linear models, which would then be costly in terms of computation time. Furthermore, the sequential model is robust to misspecification of the number of breaks, which is shown by Bai (1997). However, in this paper we only test for a single break for reasons which we discuss in Section 6.

2.4 Three-factor ATSM

Litterman and Scheinkman (1991) propose the three-factor approach in ATSMs to hedge U.S. government bonds, where the three factors are interpreted as level, steepness, and curvature of the yield curve. The authors note that, over their data set of weekly observations from January 1984 to June 1988, the likelihood-ratio test does not provide any evidence against their three-factor model. Furthermore, they find that for excess returns of zero coupon rates, with maturities varying from 6 months to 18 years, the three-factor model can explain at least 96% of the variation. This finding has led ATSMs to be estimated with three factors in, for example, Dai and Singleton (2000) and Duffee (2002).

Brennan and Xia (2002) opted for an approach with two factors, since this, on average, would lead to 96% of explained variation in term structures, using the results from Litterman and Scheinkman (1991). This has led to the KNW model being specified with two factors as well, as this model extended Brennan and Xia (2002). However, to our knowledge, the KNW model has not yet been estimated with three factors.

3 Data

We require three types of time series to be able to perform the analysis: a stock index, a price index, and bond indices at different maturities. We use a similar approach as Pelsser (2019) and Dijsselbloem et al. (2019) by estimating the model using monthly data.

We use monthly data from January 1999 until May 2021. We retrieve data from the MSCI World euro index (MSWRLDE) for the stock price index and Refinitiv three month swap interest rates at 1-10, 12, 15, 20, 25, 30 years maturity for The Netherlands (ICNLG1Y for the 1 year rate) from Datastream. We use bootstrapping to derive zero coupon bond rates from the interest rate swaps. This procedure is described in Appendix A. We obtain the price indices from the Euro area seasonally adjusted Harmonised Indices of Consumer Prices (HICP) (ICP.M.U2.Y.000000.3.INX) from the ECB.

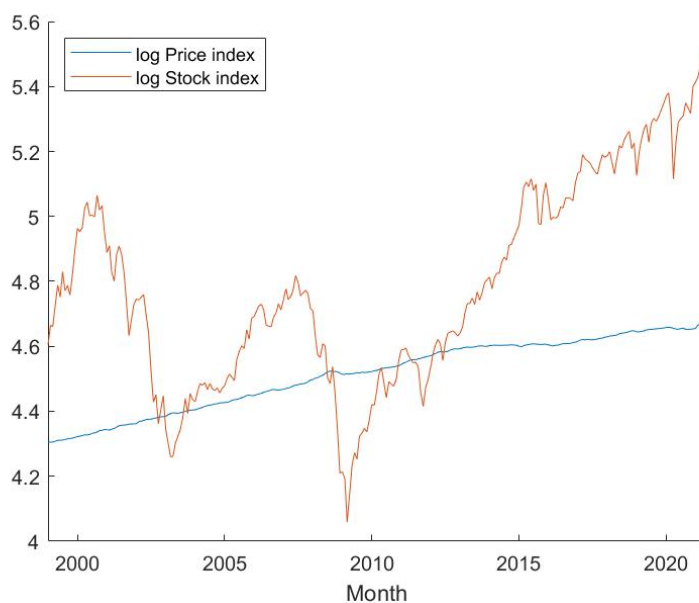


Figure 1: Natural logarithm of the HICP and MSWRLDE indices.

In the Figures 1 and 2 we show the bootstrapped Zero Coupon Bond rates and the log price and stock indices. For brevity we only show the bond maturities that are used in the estimations. We can see that the log stock index moved somewhat cyclically until December 2008, after which it shows an increasing trend. In contrast, bond rates seem to decline after December 2008. Furthermore, the log price index seems to increase fairly constantly.

We see these findings confirmed in Table 1, where we find the descriptive statistics of the first difference of the data. One interesting detail is the higher standard deviation of longer bond maturities. This could partly be caused due to the greater average decrease of bonds with longer maturities.

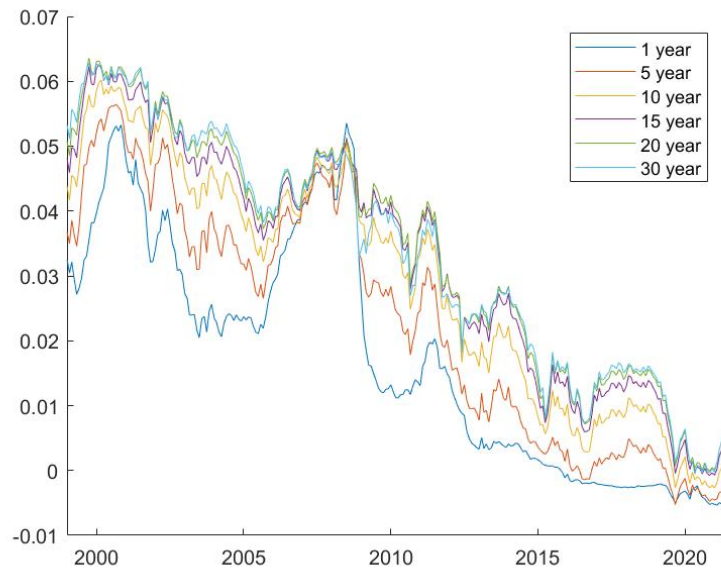


Figure 2: Zero Coupon Bond rates at different maturities.

	Mean	Standard deviation
$\Delta \ln(\text{Price Index})$	1.360	1.792
$\Delta \ln(\text{Stock Index})$	3.410	44.5
$\Delta y_t(1)$	-0.140	1.632
$\Delta y_t(5)$	-0.147	1.886
$\Delta y_t(10)$	-0.158	1.815
$\Delta y_t(15)$	-0.164	1.869
$\Delta y_t(20)$	-0.169	1.884
$\Delta y_t(30)$	-0.178	1.896

Table 1: Summary statistics of the first-differenced series ($\times 1000$).

4 Methodology

In this section we will treat the KNW model, we will explain how the Kalman Filter is applied to estimate this model, and we will explain how the parameters in this Kalman Filter are estimated. This section mainly follows the approach described in Pelsser (2019), however also draws elements from Muns (2015).

4.1 KNW model

The KNW model is an arbitrage-free and complete model, used to forecast the price index Π_t , stock index S_t , and bond indices $y_t(\tau)$, where τ denotes the maturity time of the bond. These processes are driven by instantaneous nominal interest rate r_t and instantaneous expected inflation π_t , which are affinely affected by k unobserved factors X_t :

$$dX_t = -KX_t dt + d\tilde{W}_t^{\mathbb{P}} \quad (1)$$

$$\pi_t = \delta_{0\pi} + \delta'_{1\pi} X_t \quad (2)$$

$$r_t = \delta_{0r} + \delta'_{1r} X_t \quad (3)$$

where K is a $k \times k$ matrix which ensures that the process X is mean reverting, $\tilde{W}_t^{\mathbb{P}}$ contains the first k elements from $W_t^{\mathbb{P}} \in \mathbb{R}^{k+2}$, which is a white noise term under physical measure \mathbb{P} , where the first k elements can be interpreted as uncertainty in each factor, element $k + 1$ can be interpreted as uncertainty about the unexpected inflation, and element $k + 2$ can be interpreted as uncertainty about the stock return. The δ 's are the parameters fitting X_t to r_t and π_t respectively to define an affine model.

We observe the price index and the stock index, these are assumed to follow a geometric Brownian motion. This implies that Π_t and S_t satisfy the following equations:

$$d\Pi_t = \pi_t \Pi_t dt + \Pi_t \sigma'_{\Pi} dW_t^{\mathbb{P}} \quad (4)$$

$$dS_t = (r_t + \eta_S) S_t dt + S_t \sigma'_S dW_t^{\mathbb{P}}, \quad (5)$$

where η_S denotes the stock risk premium, and both σ 's denote a $k \times 1$ vector containing their respective volatilities with respect to each element in the noise term.

The bond market is constructed using an affine term structure model. The fundamental theorem of asset pricing (e.g., Delbaen and Schachermayer, 1994) states that this market is arbitrage-free when there exists a risk neutral probability measure \mathbb{Q} , distinct from physical measure \mathbb{P} , where the price processes of traded assets are martingales. Pelsser (2019) opts for using the nominal money-market account M_t as the numéraire, where a unit would be equal to 1 currency unit being invested in a risk-free money-market account which receives the risk-free interest rate.

$$M_0 = 1, \quad dM_t = r_t M_t dt \quad \iff \quad M_t = \exp\left(\int_0^t r_s ds\right) \quad (6)$$

Since M_t is traded with a strictly positive price, this asset can be used as a numéraire. Then we can define the change of probability measure from \mathbb{P} to \mathbb{Q} via the Radon-Nikodym derivative, which is a strictly positive \mathbb{P} -martingale R_t :

$$dR_t = -R_t \lambda_t' dW_t^{\mathbb{P}}, \quad (7)$$

where λ_t is $k + 2$ dimensional vector, which ensures that R_t is a true martingale. Then we can retrieve probability measure \mathbb{Q} using $d\mathbb{Q}_t = R_t d\mathbb{P}_t$, where we can apply Girsanov's theorem in which $dW_t^{\mathbb{P}} + \lambda_t dt$ is a standard Brownian motion under probability measure \mathbb{Q} (Girsanov, 1960), since probability measure \mathbb{Q} is defined via the Radon-Nikodym derivative. This implies that the drift term $\lambda_t dt$ disappears due to the change of probability measure. However, the model is still affine when the following holds:

$$\lambda_t = \lambda_0 + \Lambda_1 X_t, \quad (8)$$

where λ_0 is a constant $k + 2$ vector and Λ_1 is a constant $(k + 2) \times k$ matrix. These can be interpreted as the state price deflator.

Now we can derive the bond prices. Under \mathbb{Q} we enforce no-arbitrage, thus all asset prices divided by M_t are martingales. In the case of a discount bond, we can derive the relative price:

$$\frac{\exp(-\tau y_t(\tau))}{M_t} = \mathbb{E}^{\mathbb{Q}} \left[\frac{1}{M_{t+\tau}} \middle| \mathcal{F} \right] \implies \exp(-\tau y_t(\tau)) = \mathbb{E}^{\mathbb{Q}} \left[\exp\left(-\int_t^{t+\tau} r_s ds\right) \middle| \mathcal{F} \right]. \quad (9)$$

In the first part of the equation we use the assumption that the price of a discount bond at maturity must be equal to one. Now we can evaluate the expectation by using a $(k + 1)$ -dimensional Ornstein-Uhlenbeck process (X_t, i_t) , where $i_t := \int_0^t r_s ds \implies di_t = r_t dt = (\delta_{0r} + \delta'_{1r} X_t) dt$. Under \mathbb{Q} we can write the dynamics of (X_t, i_t) as

$$d \begin{pmatrix} X_t \\ i_t \end{pmatrix} = \left[\begin{pmatrix} -\lambda_0 \\ \delta_{0r} \end{pmatrix} + \begin{pmatrix} -(K + \tilde{\Lambda}_1) & 0 \\ \delta'_{1r} & 0 \end{pmatrix} \begin{pmatrix} X_t \\ i_t \end{pmatrix} \right] dt + \begin{pmatrix} I_k \\ 0_{1 \times k} \end{pmatrix} dW_t^{\mathbb{Q}}, \quad (10)$$

where $\tilde{\Lambda}_1$ is the upper $k \times k$ submatrix of Λ_1 . Since this is a vector-OU process, we can derive the multivariate Gaussian distribution from this process, how this can be done is shown in Appendix C. Then the price of a discount bond

$$D_t(\tau) = \mathbb{E}_t^{\mathbb{Q}}[\exp(-(i_{t+\tau} - i_t))] = \exp(-A(\tau) - B(\tau)' X_t), \quad (11)$$

where

$$B(\tau) = (K + \tilde{\Lambda}_1)^{-1} (I_k - \exp(-(K + \tilde{\Lambda}_1)' \tau)) \delta_{1r}, \quad (12)$$

$$A(\tau) = \int_0^t \delta_{0r} - \lambda_0' B(s) - \frac{B(s)' B(s)}{2} ds. \quad (13)$$

Since the parameters are assumed to be constant in this model, $A(\tau)$ and $B(\tau)$ only depend on the maturity τ and $D_t(\tau)$ only depends on τ and X_t . Now we can return to (9) and define the zero-coupon rate:

$$y_t(\tau) = \frac{\ln D_t(\tau)}{-\tau} = \frac{A(\tau)}{\tau} + \frac{B(\tau)'}{\tau} X_t, \quad (14)$$

in which we can confirm that the zero coupon rate is affine in the factors.

We then move on to construct the stock market. Due to no-arbitrage, $\frac{S_t}{M_t}$ is a martingale under \mathbb{Q} with dynamics

$$d\frac{S_t}{M_t} = (\eta_S - \sigma'_S(\lambda_0 + \Lambda_1 X_t))\frac{S_t}{M_t}dt + \frac{S_t}{M_t}\sigma'_S dW_t^{\mathbb{Q}}. \quad (15)$$

The second term on the right hand side has mean 0 due to the Brownian motion, this means that the first term should also have mean 0 for the process to be a martingale, which leads to the following restrictions on λ_0 and Λ_1 under \mathbb{Q} :

$$\sigma'_S \lambda_0 = \eta_S, \quad \sigma'_S \Lambda_1 = 0. \quad (16)$$

However, since we use the \mathbb{P} -dynamics of S_t and Π_t in our estimation of the KNW model, the restrictions in (16) are not required (Pelsser, 2019).

4.2 Kalman Filter in the KNW model

We augment the state vector such that $\tilde{X}_t = (X'_t, \ln \Pi_t, \ln S_t)'$. This allows us to combine (4), (5), and (14), where its dynamics under measure \mathbb{P} are

$$d\tilde{X}_t = \left[\begin{pmatrix} 0_{1 \times k} \\ \delta_{0\pi} - \frac{1}{2}\sigma'_{\Pi}\sigma_{\Pi} \\ \delta_{0r} + \eta_S - \frac{1}{2}\sigma'_S\sigma_S \end{pmatrix} + \begin{pmatrix} -K & 0_{k \times 2} \\ \delta'_{1\pi} & 0_{1 \times 2} \\ \delta'_{1r} & 0_{1 \times 2} \end{pmatrix} \begin{pmatrix} X_t \\ \ln \Pi_t \\ \ln S_t \end{pmatrix} \right] dt + \begin{pmatrix} [I_k 0_{k \times 2}] \\ \sigma'_{\Pi} \\ \sigma'_S \end{pmatrix} dW_t^{\mathbb{P}}. \quad (17)$$

This system of equations can be written in the form $d\tilde{X}_t = (a + A\tilde{X}_t)dt + CdW_t$, which can be interpreted as a Ornstein-Uhlenbeck process. After deriving the transition density, which can be found in Appendix C, we can write the system in VAR(1) form as

$$\tilde{X}_t = \phi + \Phi\tilde{X}_{t-\Delta t} + \epsilon_t \quad Var[\epsilon_t] = Q, \quad (18)$$

where

$$\phi = \int_0^{\Delta t} \exp(Au)adu, \quad \Phi := \exp(A\Delta t), \quad Q := \int_0^{\Delta t} \exp(Au)CC' \exp(A'u). \quad (19)$$

We define the measurement equation of the Kalman Filter as follows:

$$\tilde{y}_t = \begin{pmatrix} y_t \\ \ln \Pi_t \\ \ln S_t \end{pmatrix} = a + B\tilde{X}_t + \eta_t \quad Var[\eta_t] = H, \quad (20)$$

where y_t is a vector containing the zero bond coupon rates with different maturities, coefficients a and B are defined in (21) and η_t is an i.i.d. multivariate normal noise term with mean 0 and variance H , defined in (22).

$$a := \begin{pmatrix} A(\tau_1)/\tau_1 \\ \vdots \\ A(\tau_m)/\tau_m \\ 0 \\ 0 \end{pmatrix} \quad B := \begin{pmatrix} B(\tau_1)/\tau_1 & 0 & 0 \\ \vdots & \vdots & \vdots \\ B(\tau_m)/\tau_m & 0 & 0 \\ 0_{1 \times k} & 1 & 0 \\ 0_{1 \times k} & 0 & 1 \end{pmatrix}, \quad (21)$$

where $B(\tau) = (K + \Lambda_1)'(I - \exp(-(K + \Lambda_1)' * \tau))\delta_{1r}$ and $A(\tau) = \int_0^\tau B(s)ds$. Here we follow the approach of Muns (2015), which has derived a closed form solution for $A(\tau)$ and $B(\tau)$, exploiting the fact that this market model does not reward taking unexpected inflation risk. These equations can be found in Appendix B.

For H , we assume that there exists no error in the observation of the price and stock indices, leading to the two bottom rows to be zero rows. Furthermore, we assume that there is no cross-correlation in the errors of the bond yields across different maturities, however variances of different maturities are allowed to vary.

$$H := \begin{pmatrix} \text{diag}(h_m^2) & 0_{m \times 2} \\ 0_{2 \times m} & 0_{2 \times 2} \end{pmatrix}. \quad (22)$$

Combining (18) and (20) leads us to the following distribution, which can be estimated via a Kalman Filter:

$$f \left(\begin{pmatrix} \tilde{X}_t \\ \tilde{y}_t \end{pmatrix} \middle| \tilde{X}_{t-\Delta t} \right) \sim N \left(\begin{pmatrix} \phi + \Phi \tilde{X}_{t-\Delta t} \\ a + B(\phi + \Phi \tilde{X}_{t-\Delta t}) \end{pmatrix}; \begin{pmatrix} Q & QB' \\ BQ & BQB' + H \end{pmatrix} \right). \quad (23)$$

We do not observe the state $\tilde{X}_{t-\Delta t}$ exactly. However, the Kalman Filter allows us to find an estimated state, $\hat{X}_{t-\Delta t}$, of which we can construct the conditional distribution:

$$f(\tilde{X}_t | \hat{X}_{t-\Delta t}) \sim N(\phi + \Phi \hat{X}_{t-\Delta t}; P_{t|t-\Delta t}), \quad P_{t|t-\Delta t} := \Phi P_{t-\Delta t} \Phi' + Q, \quad (24)$$

where $P_{t|t-\Delta t}$ is the conditional variance, based on the information set at $t - \Delta t$ ($\mathcal{I}_{t-\Delta t}$).

This allows us to rewrite (23) into:

$$f \left(\begin{pmatrix} \tilde{X}_t \\ \tilde{y}_t \end{pmatrix} \middle| \hat{X}_{t-\Delta t} \right) \sim N \left(\begin{pmatrix} \phi + \Phi \hat{X}_{t-\Delta t} \\ a + B(\phi + \Phi \hat{X}_{t-\Delta t}) \end{pmatrix}; \begin{pmatrix} P_{t|t-\Delta t} & P_{t|t-\Delta t} B' \\ B P_{t|t-\Delta t} & V_t \end{pmatrix} \right), \quad (25)$$

where $V_t := B P_{t|t-\Delta t} B' + H$. We observe \tilde{y}_t at time t , this allows us to compute the conditional distribution of \tilde{X}_t , given $\tilde{y}_{t-\Delta t}$ and $\hat{X}_{t-\Delta t}$, using:

$$f(\tilde{X}_t | \tilde{y}_t, \hat{X}_{t-\Delta t}) \sim N(\phi + \Phi \hat{X}_{t-\Delta t} + K_t u_t; P_t), \quad (26)$$

where

$$u_t := \tilde{y}_t - (a + B(\phi + \Phi \hat{X}_{t-\Delta t})), \quad (27)$$

$$K_t := P_{t-\Delta t} B' V_t^{-1}, \quad (28)$$

$$P_t := P_{t|t-\Delta t} - P_{t|t-\Delta t} B' V_t^{-1} B P_{t|t-\Delta t} = (I - K_t B) P_{t|t-\Delta t}, \quad (29)$$

where u_t can be interpreted as a regression error. K_t is introduced for ease of notation and is the Kalman Gain, this can be seen as the increase in efficiency by knowing \tilde{y}_t . P_t is the conditional variance, when \tilde{y}_t is known. From the multivariate normal distribution given \tilde{y}_t , we can derive the conditional expectation:

$$\hat{X}_t := \mathbb{E}[\tilde{X}_t | \tilde{y}_t, \hat{X}_{t-\Delta t}] = \phi + \Phi \hat{X}_{t-\Delta t} + K_t u_t. \quad (30)$$

This completes the calculation of the current time step of the Kalman filter, now we are able to iterate forward over all t in the data, as long as we have a starting point for the state variable X and the parameters. This will be treated in the next subsection.

4.3 Parameter estimation

From (25) we can deduce

$$f(\tilde{y}_t | \hat{X}_{t-\Delta t}) \sim N(a + B(\phi + \Phi \hat{X}_{t-\Delta t}); V_t), \quad (31)$$

this implies

$$\ln(L_t) = -\frac{d}{2} \ln(2\pi) - \frac{1}{2} \ln(|V_t|) - \frac{1}{2} u_t' V_t^{-1} u_t, \quad (32)$$

where d is the amount of dimensions in the multivariate normal, which in this case is equal to $m + 2$.

To solve this system however, we require an initialization of the Kalman Filter for \hat{X}_0 and P_0 . This can be done in multiple ways, however in our paper we will apply two methods of initialization, following Pelsser (2019), which uses the diffuse prior and the stationary prior.

The diffuse prior sets initial conditional variance $P_0 = I_{(k+2) \times (k+2)}$ and initial state $\hat{X}_0 = 0_{k \times 1}$. Using this approach requires us to delete the first two observations to account for two non-stationary variables in \tilde{X} , being $\ln(\Pi_t)$ and $\ln(S_t)$. Thus we need to minimize the sum of the negative log-likelihoods using the parameters

$$\theta = \arg \min_{\theta} \sum_{t=3}^T -\ln(L_t). \quad (33)$$

This approach does require some caution, as Pelsser (2019) retrieved non-stationary results in this case, which would be undesirable in practice. This has led us to penalizing non-positive and non-real eigenvalues of $M = (K + \tilde{\Lambda}_1)'$ in the likelihood function by giving those outcomes a high and positive value in the calculation of the negative log-likelihood, ensuring that this parameter set is not selected.

The stationary prior assumes that we can observe the non-stationary variables $\ln(\Pi_t)$ and $\ln(S_t)$ without measurement error. Then we can set $\hat{X}_0 = (E[X_\infty]', \ln(\Pi_0), \ln(S_0))'$ and $P_0 := \begin{pmatrix} Var[X_\infty] & 0_{k \times 2} \\ 0_{2 \times k} & 0_{2 \times 2} \end{pmatrix}$, where $E[X_\infty]$ and $Var[X_\infty]$ are respectively the unconditional mean and variance of X , subscript 0 is in this case the first observation after removing the first two observations to account for the two non-stationary variables. The unconditional mean of X is $0_{k \times 1}$ by construction, while the unconditional variance of X is defined as

$$vec(Var[X_\infty]) = (I_{k^2} - K \otimes K)^{-1} vec(I_k), \quad (34)$$

where \otimes denotes the Kronecker product, and $vec(\cdot)$ denotes the vectorization operator (Lütkepohl, 2005). We will minimize from $t = 4$ onward, as we do not minimize over the initial state and drop an extra observation, since that is used as input for the initial state, following Pelsser (2019). This leads to the following minimization of the negative log-likelihood:

$$\theta = \arg \min_{\theta} \sum_{t=4}^T -\ln(L_t). \quad (35)$$

5 Extensions

5.1 Structural breaks

We test for structural breaks in the Kalman Filter using a SupLR test, which is an extension of the likelihood-ratio test where the change point is known and asymptotically follows a chi-squared distribution (Wilks, 1938). Andrews (1993) proposes the SupW, SupLM and SupLR tests, which test structural change in a model with a single unknown change point t . We opt for the SupLR test due to the SupW and SupLM tests being asymptotically equivalent to the SupLR test under suitable assumptions (Andrews, 1993) and its ease of use, as the log-likelihood values are already calculated in the Kalman Filter. Andrews (1993) finds that the asymptotic distributions of these tests are nonstandard, since the change parameter does not exist under the null hypothesis, and finds an asymptotic null distribution for the null hypothesis. Approximations of the distributions of the null hypothesis for finite samples are given in, e.g., Diebold and Chen (1996), which propose approximations based on asymptotics and bootstrapping. When testing for a structural break, we test null hypothesis $H_0 : \theta_1 = \theta_2$ against alternative hypothesis $H_a : \theta_1 \neq \theta_2$, where θ_1 is used as the parameter set before the presumed break moment t and θ_2 as the parameter set after the presumed break moment t and θ_0 is the parameter set estimated over the full sample.

The SupLR statistic is defined as the supremum over a series of likelihood-ratio statistics:

$$SupLR = \sup_t LR(t). \quad (36)$$

The likelihood-ratio statistic is defined in this case as

$$LR(t) = 2 \left[\max_{\theta_1} \ln L_{1,\dots,t}(\theta_1) + \max_{\theta_2} \ln L_{t+1,\dots,T}(\theta_2) - \max_{\theta_0} \ln L_{1,\dots,T}(\theta_0) \right], \quad (37)$$

where $L_{t_1,\dots,t_2}(\theta) = \sum_{i=t_1}^{t_2} L_i(\theta)$, see for example Wilks (1938). We can construct quantiles of the statistic via bootstrapping. We do this by generating samples of the same length of time series using (25), sampling from the multivariate normal under the null where no breaks happen, similar to Morley et al. (2011). This allows us to generate SupLR statistics under the null hypothesis, which allows us to test the statistical significance of the assumed break in the data.

In practice it is advisable to apply some sort of symmetric trimming of the computation of test statistics to keep the sizes of the subsamples sufficiently large. In this case we opt for a symmetric trimming of 30%, leading to $0.3T < t < 0.7T$, due to the amount of parameters in the model that we need to estimate. Furthermore, Diebold and Chen (1996) find that for an AR(1) model the distribution of the null hypothesis found in Andrews (1993) shows diminishing power of the test statistic once the location of the break moves to the edge of the sample, motivating the use of trimming.

In theory, we would apply a sequential approach in the case that we find a structural break. This entails splitting the sample in two subsamples, one before break period t and one after break

period t and repeating the approach of finding a break within these subsamples. In practice however, we see in Section 6 that searching for a second break may lead to practical issues.

5.2 Introduce third factor in X

The Federal reserve in the US uses three factors in their factor models to estimate the zero coupon bond rate (Kim and Wright, 2005), this also gives us the three factors to interpret as in Litterman and Scheinkman (1991), i.e., the first, second and third factors can be interpreted as the level, slope and curvature of the zero coupon curve, respectively, instead of just the level and the slope in the two-factor model. Furthermore, we can use the goodness of fit measures to observe whether the addition of the third factor would be desirable. Additionally, we can observe whether the parameter estimates in a three-factor model would differ significantly from the results that the DNB and Pelsser (2019) found. Furthermore, we can run simulations in which we can observe to what extent the increase in factors would lead to a different scenario set.

To assess whether the goodness of fit increases when introducing the third factor, we can use the Bayesian and Akaike Information Criteria (BIC and AIC, respectively), devised by Schwarz (1978) and Akaike (1974) respectively. These information criteria are defined as follows:

$$BIC = k \ln(n) - 2 \ln(L), \quad (38)$$

$$AIC = 2k - 2 \ln(L), \quad (39)$$

where k is the number of parameters that have to be estimated, n is the amount of observations in the sample, and $\ln(L) = \sum_t \ln(L_t)$, where $\ln(L_t)$ is the log-likelihood calculated in (32).

6 Results

In this section we will discuss the results of the paper. Firstly, we will look at the two-factor case and test for a structural break. Then we will look at the three-factor case and test for a structural break, after which we compare the two- and three-factor models using the AIC and BIC. Concluding this section, we will look at the economic relevance of the analysis by generating scenarios that result from these parameters.

6.1 Two-factor model estimations

As a starting point for the estimations, we use the parameters from DNB in Pelsser (2019). Then we run constrained optimization (fmincon in MATLAB Optimization Toolbox (2020)) twice, where the second run receives the parameters from the previous optimization, to retrieve estimated parameters for the diffuse prior. For the stationary prior, we use the estimated parameters for the diffuse case as an initial value for fmincon. We use this approach due to an issue with a local minimum if we follow the same procedure as in the diffuse case. The results from these estimations can be seen in Table 4 in Appendix D. We find seemingly similar values for both initializations of the prior. However, due to the large amount of parameters it would be more useful to look into generated scenarios in Section 6.6.

6.2 Testing for a structural break using two factors

We obtain likelihood-ratio statistics by using the parameters from Section 6.1 as the initial values in the optimization routine. This results in the two parameter sets for the first candidate break point from 1 to t_1 , and $t_1 + 1$ to T , where t_1 is the first candidate break point equal to the rounded value of $0.3 * 269 \simeq 81$. From there on, we use the lowest negative likelihood resulting from the starting parameter sets calculated in Section 6.1 and the parameters of the previous candidate break point as initial values. Then we repeat this process but reverse the order in which we perform the calculations i.e., starting from the end of the set of candidate break points to the beginning of the set of candidate break points. This aids in finding lower values for the negative log-likelihood. Bootstrapped SupLR statistics are found by generating a series under the null hypothesis, then we repeat the same procedure as in generating the SupLR values on the data. However, in this case we only use the parameter set from the previous candidate break point as initial value for the optimization to reduce computation time. This process is repeated 100 times, leading to 100 SupLR statistics.

The obtained LR-statistics are shown in Figure 3. We see that we obtain similar results in both cases, with both series showing a fairly sharp peak reminiscent of a shark fin, which is a sign of a strong single break. However, we find our SupLR statistics at different points in time: In the diffuse case we find a SupLR statistic of 825.04 in October of 2008, while we find a SupLR statistic of 823.02 in September of 2008. The parameters found until and after their respective break points are shown in Tables 5 and 6 in Appendix D. In our bootstrapped simulations we find a 95th percentile has a SupLR statistic of 86.37, with a maximum of 108.30

in the diffuse case. In the stationary case we find that the 95th percentile of the bootstrapped SupLR statistics is 70.22, with a maximum of 93.63. The histograms of these bootstrapped SupLR statistics can be found in Figures 8 and 9 in Appendix E. Thus, we find that we can reject the null hypotheses for both cases, as both SupLR statistics exceed the critical value of the distribution of the bootstrapped null hypothesis at the 5% significance level.

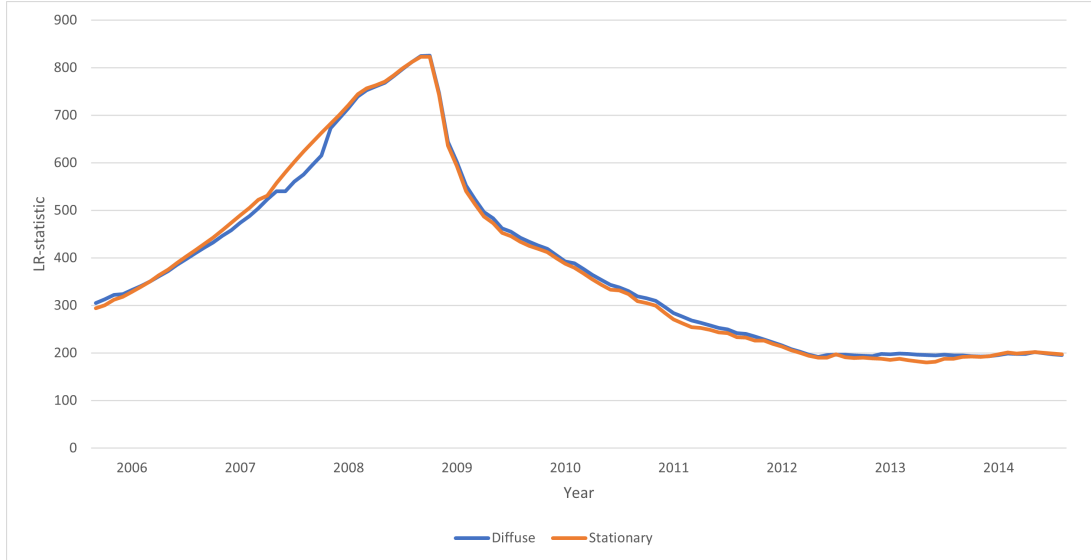


Figure 3: Likelihood-ratio statistics of the two-factor model.

Due to issues regarding local minima, we do not show results of a potential second break.

6.3 Three-factor model estimations

To obtain an initial value for the optimization with added parameters, we sample all parameters from a uniform distribution between twice the value of previously found optimal parameters for the two-factor case and 0, with extra parameters being filled in such that no complex values are returned. For the diffuse approach, we sample 50000 times from this uniform distribution, of which we select the 4 lowest resulting negative log-likelihoods, again discarding the log-likelihoods with a complex component. These 4 parameter sets are then used as initial values for our optimization, where we run `fmincon` with these initial values and run `fmincon` once again with the resulting parameter sets of this optimization and then pick the lowest negative log-likelihood. For the stationary approach, we copy the starting value of the diffuse approach and run `fmincon` twice, using the parameters resulting from the first optimization in the second run of `fmincon`. The resulting parameters of these estimations can be found in Table 7 in Appendix D. We will look at the practical implications of these parameter sets in Section 6.6.

6.4 Testing for a structural break using three factors

We calculate LR-statistics following the method described in Section 6.2. The obtained LR-statistics are shown in Figure 4. We see that we obtain different shapes in the LR-statistics.

We find in the case of the diffuse prior that there is a build-up towards a certain peak in June of 2008, which is very quickly followed up by a higher peak which contains the SupLR statistic of 700.04 in October of 2008, after which we find a fast decrease until December of 2008. The values of the LR-statistics then increase towards April of 2009 and subsequently seems to decline rather steadily. By contrast, we see that the LR-statistics in the stationary case shows a sharper break and a much higher value of the SupLR statistic in October of 2008 with value 1047.63. The series starts off on a higher level and follows a similar trend as the diffuse case, showing a small peak in respectively February and March of 2007 in the diffuse and stationary cases. The LR-statistics also show a similar steep decline after October of 2008 until January of 2009, followed by a relatively small increase, which then declines steadily. The resulting parameter sets can be found in Tables 8 and 9 in Appendix D.

We find that both SupLR statistics are statistically significant at the 5% level, since these statistics exceed the 95th percentile of the bootstrapping under the null with 100 runs in both cases, being 38.28 and 38.58 for the case with the diffuse and stationary priors respectively. The histograms of the bootstrapped SupLR statistics can be found in Figures 10 and 11 in Appendix E. Therefore, we may reject the null hypothesis of having no structural break in the parameters in the full sample at the 5% significance level.

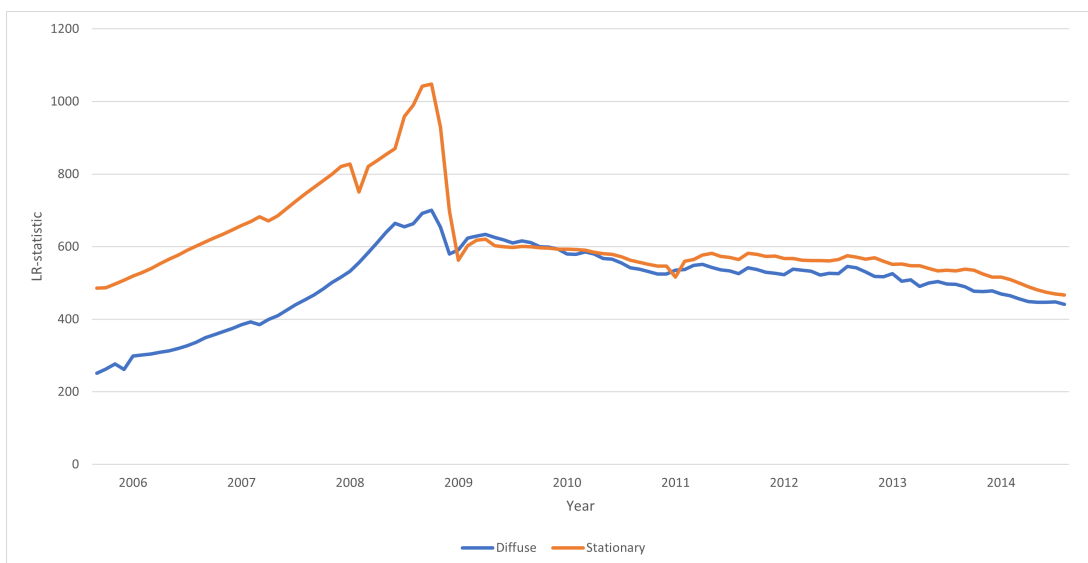


Figure 4: Likelihood-ratio statistics of the three-factor model.

We will not continue the analysis for further breaks in the three-factor case, due to the relatively small number of data points per parameter in the two subsamples that arise from both break points.

6.5 Comparing the two- and three-factor models

We use the Bayesian and Akaike Information Criteria defined in (38) and (39). The two-factor model contains 29 parameters, while the three-factor model contains 42 parameters, giving us k for both models. The time series contains 269 observations, this is equal for both models, giving

us the value for n after this has been corrected for the number of observations that are excluded in the likelihood function. We can see in Table 2 that we prefer the three-factor model in both the diffuse and stationary case due to lower AIC and BIC values. Note that it is not desirable to compare the diffuse and stationary priors across each other due to the exclusion of an extra data point in the stationary case.

	Two-factor model		Three-factor model	
	Diffuse prior	Stationary prior	Diffuse prior	Stationary prior
AIC	-24076.88	-23994.82	-24249.28	-24174.68
BIC	-23972.85	-23890.90	-24098.62	-24024.01

Table 2: AIC and BIC values for the two- and three-factor model, using the full sample.

Moreover, we show the AIC and BIC values, using the sample after October 2008 with their respective obtained parameter sets, obtained in Sections 6.2 and 6.4, in Table 3. We once again see that we would prefer the three-factor models for both priors due to lower values of both the AIC and BIC. Note that in this case we do not have differing values for n , as we sum the likelihoods from November 2008 onwards, however as the stationary case needs to exclude an extra data point, we have given this extra information, which again might not lead to a fair comparison between the diffuse and stationary priors.

	Two-factor model		Three-factor model	
	Diffuse prior	Stationary prior	Diffuse prior	Stationary prior
AIC	-13816.04	-13811.26	-13943.25	-14025.40
BIC	-13903.54	-13898.76	-14069.98	-14152.12

Table 3: AIC and BIC values for the two- and three-factor model after October 2008.

6.6 Economic relevance of the results

We run a simulation of 10000 runs using each estimated parameter set. This is done using Equation (25) for a length of 720 months (equal to the 60 years that need to be simulated in the achievability test by DNB). Below we see the results from the generated scenario sets. To compare our results, we also include the unrestricted stationary and DNB parameters, found in Pelsser (2019), where we only include the DNB parameters in the graphs in the main text for clarity. We omit the diffuse case from Pelsser (2019), because the values for price and stock index explode due to non-stationary results for X . The mean of the simulated 1-, 10-, 20-, and 30-year ZCB rates are shown together with the log price and stock indices in Figures 5, 6, and 7, where we show the results from the DNB parameters as a reference in each set of figures. Furthermore, we show the individual means and 5th percentiles of scenarios in Appendix H, where also the scenarios for the 5-, and 15-year ZCB rates are shown. Note that the scenarios in the Appendix have been run with a different seed, leading to different outcomes. This is done to

show the effects of the non-stationarity of \tilde{X} , as the eigenvalues of Φ are not guaranteed to lie within the unit circle under the current assumptions. The eigenvalues of Φ are shown in Tables 12, 13, and 14 in Appendix G.

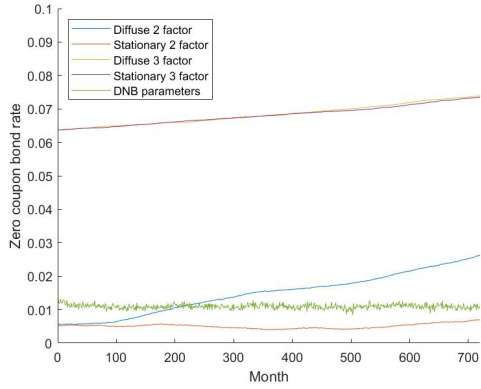
From Figure 5 we see the mean of the scenarios for the ZCB rates, and the log price and stock indices, using the parameters estimated on the full sample for both specifications of the two- and three-factor model. We find that the mean log stock indices show negative values in both specifications of the two-factor model and that the diffuse case of the two-factor model shows some non-stationarity, with the ZCB rates drifting upwards. Furthermore, we find that, on average, the three-factor model specifications show very similar results.

In Figure 6 we see the mean of the scenarios for the ZCB rates, and the log price and stock indices, using the parameters estimated on both specifications of the two-factor model before and after the observed break. We observe negative log stock indices, which aligns with the descriptive statistics before the break, seen in Table 10 of Appendix F. Furthermore, the price and stock indices after the break are very similar, to the point that this might not be easily distinguished when looking at the figure. Lastly, we observe that the simulated ZCB rates using the parameters after the break are lower when compared to the same model specification on both the full sample and the sample before the break.

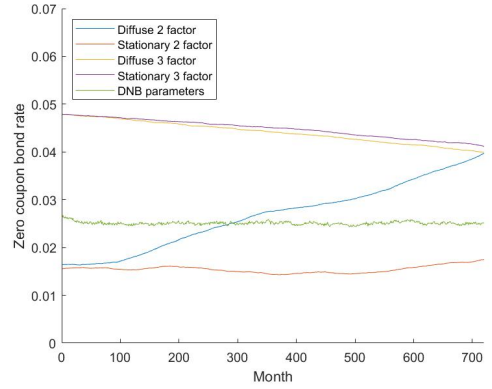
In Figure 7 we see a similar figure, now using the parameters estimated on both specifications of the three-factor model before and after the observed break. We can draw similar observations as in the two-factor case, where the ZCB rates are lower when using the parameters estimated after the break. However in this case we see relatively little similarity in the log price and stock indices after the break. A peculiar point is that the mean log stock indices from the parameters estimated before the break are not negative, deviating from the average decrease that we find in the data.

When looking at these figures overall, we see some slight trending in the two- and three-factor models in Figure 5. This can be explained by the eigenvalues of Φ , which can be seen in the tables of Appendix G, which determines whether \tilde{X} is stationary. We also notice that our estimations always underestimate the price index when compared to the DNB scenario set and that in cases incorporating the break we also find lower stock indices. In the three-factor model, we see that the ZCB rates on average shows some form of an inverted yield curve in all cases.

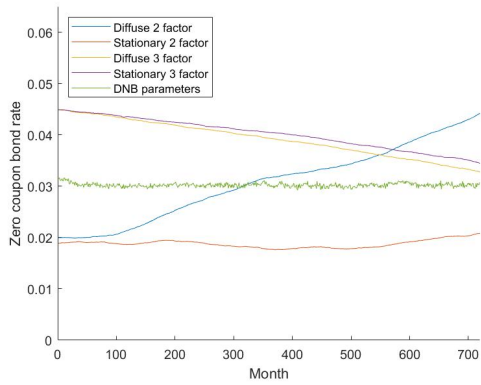
In Appendix H, we see some different values of the models which have non-stationary \tilde{X} , this can be seen clearly in Table 12, where on average the ZCB rates trend downward. Furthermore, some idea of the volatility of the scenarios can be found when comparing the levels of the 5th percentiles to the means. However, we will not discuss this to avoid an enumeration of model specifications with different levels of volatility.



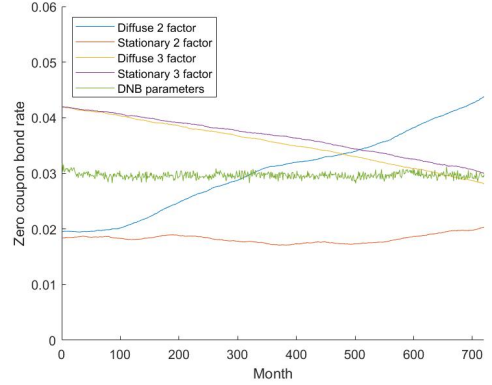
(a) 1-year Zero Coupon Bond rates



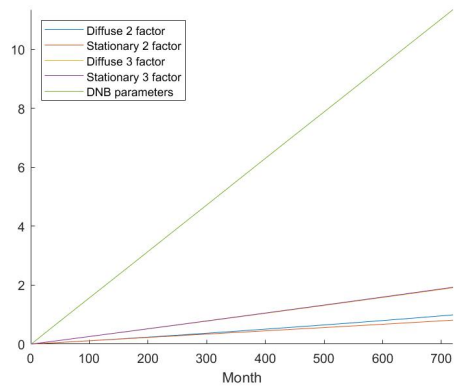
(b) 10-year Zero Coupon Bond rates



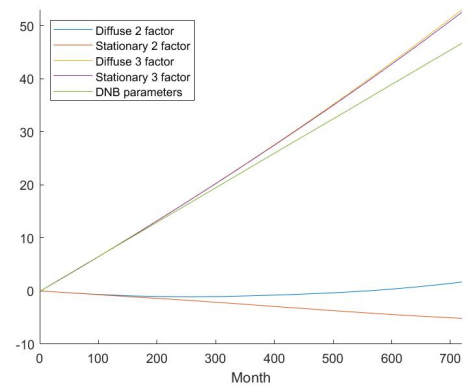
(c) 20-year Zero Coupon Bond rates



(d) 30-year Zero Coupon Bond rates

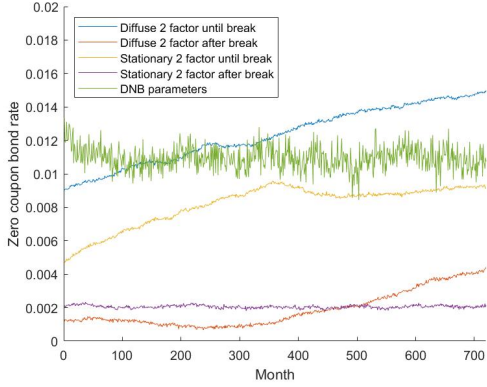


(e) Log Price Index

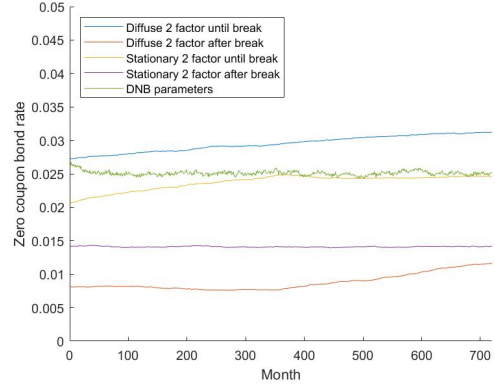


(f) Log Stock Index

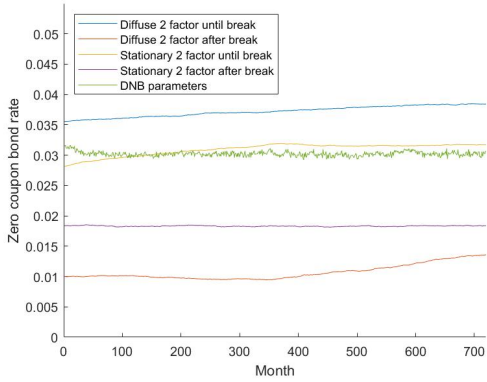
Figure 5: Mean of scenarios from full sample estimations



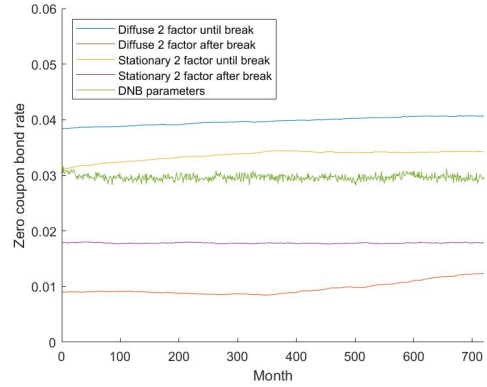
(a) 1-year Zero Coupon Bond rates



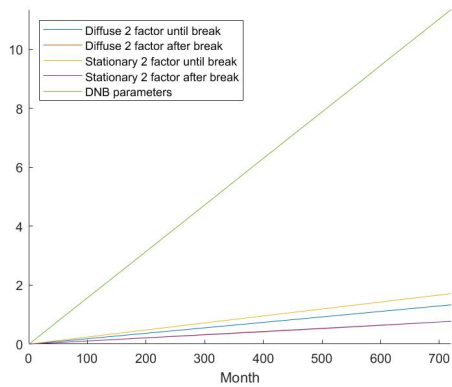
(b) 10-year Zero Coupon Bond rates



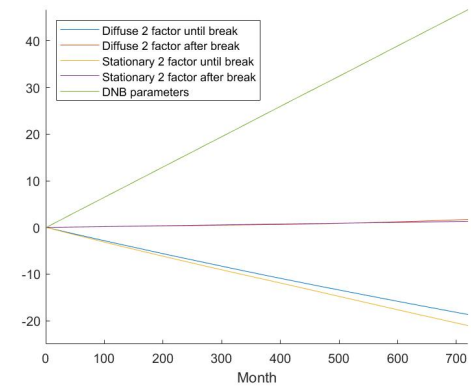
(c) 20-year Zero Coupon Bond rates



(d) 30-year Zero Coupon Bond rates

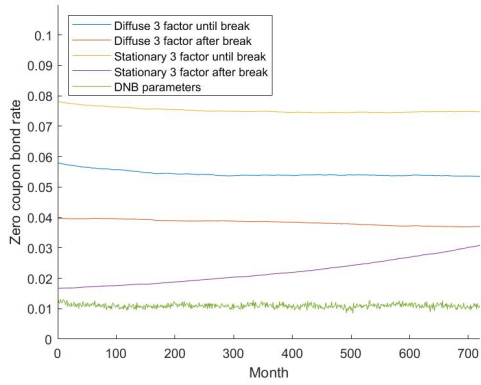


(e) Log Price Index

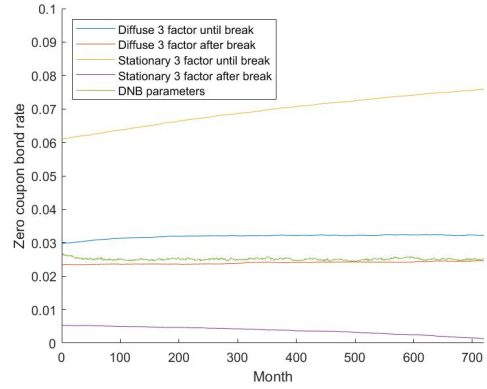


(f) Log Stock Index

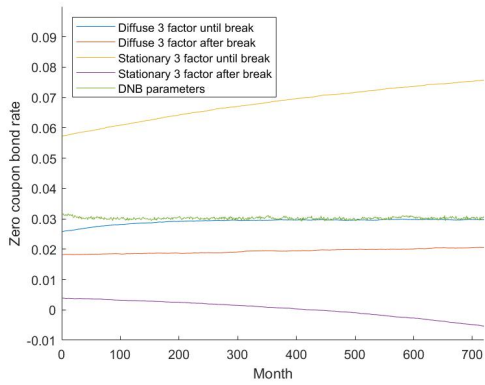
Figure 6: Mean of scenarios from two-factor split sample estimations



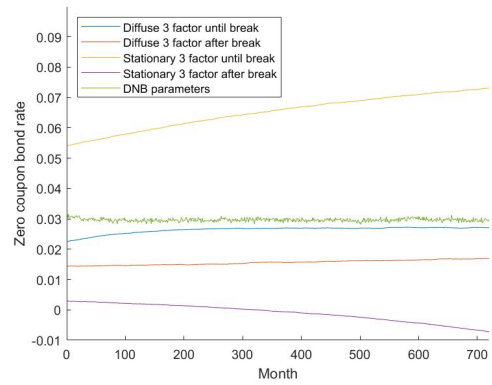
(a) 1-year Zero Coupon Bond rates



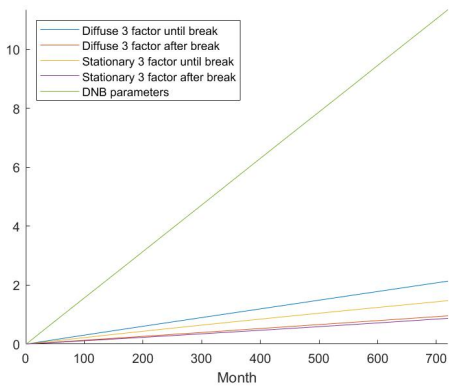
(b) 10-year Zero Coupon Bond rates



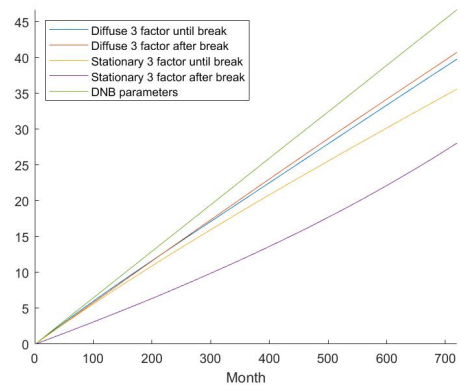
(c) 20-year Zero Coupon Bond rates



(d) 30-year Zero Coupon Bond rates



(e) Log Price Index



(f) Log Stock Index

Figure 7: Mean of scenarios from three-factor split sample estimations

7 Discussion

In this paper we have tested for structural breaks and found an increase in fit in introducing a third factor in the KNW model using data starting in January 1999 to May 2021. We find statistical evidence for a structural break in both the two-, and three-factor KNW model for both specifications of the prior. Moreover, using the parameters maximizing the log-likelihood on the full sample may give scenarios which on average do not seem to align with the descriptive statistics. This can be seen in, for example, the negative log stock indices in the two-factor model. This issue seems to be mitigated by estimating the model using the subsample after the found break point. Furthermore, we find in the estimations on the full sample that there is an increase in fit using the three-factor model when compared to the two-factor model, using the AIC and BIC values resulting from the models. This finding is robust to the found break, as applying the model parameters estimated after the found break on the data after October 2008 also gives us preference for the three-factor model using the AIC and BIC. Lastly, we find that the implementation of the breaks give rise to differing scenarios, leading to lower ZCB rates in the scenarios that use parameters estimated after the break. This could be of practical use, as the parameters are currently calibrated to give rates that align with their expectations. However, decreasing the sample size such that the break is excluded may already alleviate the need of calibration due to the lower found rates after the break.

The timings of the break points are all found in the aftermath of the financial crisis of 2007. Three of the four models indicate breaks in the parameters in October of 2008, while the remaining model indicates a structural break in September of 2008. The break in October seems to align with the introduction of fixed-rate full allotment policy by the ECB, while the break in September can be attributed to that month being one of the critical months in the financial crisis, where for example Lehman Brothers went bankrupt with severe effects for the financial sector.

An interesting point of discussion is the economic relevance of the results. We see that there are many specifications which would fit the data well, however some specifications may give somewhat unrealistic results, which do not seem to represent the trends found in the data. For example, we see scenarios in which the stock indices decrease rather heavily, while the stock market increased on average in the data. This might suggest that the model might give more weight towards optimizing for the bond rates. It could be interesting for future research to analyze the sensitivity of the results in the KNW model to the amount of bond maturities that are included in the Kalman Filter.

Additionally, we find that the eigenvalues of Φ are not forced to be inside the unit circle, leading to non-stationary \tilde{X} . This is likely to not be desirable in practice. Thus, future research can analyze the effects of constraints on Φ , such that \tilde{X} remains stationary and to what extent the current non-stationarity affects the scenarios.

Moreover, we find that while there might not be seemingly large differences between parameter sets that these still can give fairly different outcomes in the scenario's that result from these.

Therefore, it might be of practical use for DNB to test the sensitivities of the scenarios to each parameter and explain the implications of a quarterly change in certain parameters to increase transparency towards pension funds that need to perform these tests.

One setback in the writing of the paper was that the estimation of further breaks in the three-factor model was not desirable, as many parameters need to be estimated, while having relatively few data points in the subsample. Future research may attempt to update this when sufficient data will be available. Another issue we came across was the encounter of local minima in some cases of the estimation of further breaks in the two-factor model. The parameter set under the null hypothesis would lead to local minima in the bootstrapping of SupLR statistics. This led us to omit these results, as this might decrease the clarity of the paper. This issue also showcases that we find the common challenge of encountering difficulties with estimating no-arbitrage models. See for example Kim (2007), which found that difficulties in estimation arise due to the large amount of parameters and the nonlinear relationship between the parameters and yields.

Lastly, we have not studied the regularity conditions of this problem. This might raise some issues regarding optimality of the structural break testing in this paper, as Andrews and Ploberger (1994) have shown that likelihood-ratio tests are not optimal when the regularity conditions do not hold. In that case a weighted average power criterion can be used, which is optimal and converges to LM-, Wald- and LR-tests when the regularity conditions hold. However, to demarcate the problem and have the thesis feasible within the allotted time, we opted for the SupLR test. This opens the avenue for further research to check the regularity conditions of this problem and apply the weighted average power criterion if needed.

A Bootstrapping swaps to zero coupon bonds

To calculate the zero coupon bonds from the interest rate swaps (IRS) collected in Section 3 we use bootstrapping, following Dijsselbloem et al. (2019). Since we obtained the IRS from the first 10 years, we can apply a direct method to obtain the zero coupon rates for these years. For the first year we need to solve

$$\frac{1 + r_1}{1 + z_1} = 1, \quad (40)$$

where r_1 and z_1 are respectively the swap and zero coupon rates with a one year maturity. Solving this equation simply leads to $z_1 = r_1$, extending this to longer maturities requires us to solve the following

$$\sum_{t=1}^{\tau-1} \frac{r_\tau}{(1 + z_t)^t} + \frac{1 + r_\tau}{(1 + z_\tau)^\tau} = 1. \quad (41)$$

The equation arises due to the nature of the IRS cashflows, returning interest rate r_τ at each time period and returning the principal, which we set at 1, at maturity. These cashflows are discounted at each time period t with the zero coupon rate z_t to the power of t to calculate a net present value of the IRS. Since the principal is set to 1, the net present value of the IRS should also be set to 1 (the principal) due to no-arbitrage. Solving (41) gives us

$$z_\tau = \frac{1 + r_\tau}{1 - \sum_{t=1}^{\tau-1} \frac{r_\tau}{(1+z_t)^t}}^{\frac{1}{\tau}} - 1. \quad (42)$$

Note that this requires $z_{\tau-1}$ and previous to calculate z_τ . Since our data set also contains the 12, 15, 20, 25, and 30 year IRS, we cannot use (42) due to the gaps in time. Therefore, we use the forward rate to help us calculate the zero coupon rates. We define the one year forward rate as follows:

$$f_{t,t+1} = \frac{(1 + z_{t+1})^{t+1}}{(1 + z_t)^t} - 1. \quad (43)$$

Then we make the assumption that the one year forward rates between two observed maturities are constant:

$$f_{t,t+1} = f_{t+1,t+2}, \quad \forall t, \tau_1 \leq t < \tau_2, \quad (44)$$

where we define τ_1 and τ_2 as two maturities, which are contained in our data set. As the rates between τ_1 and τ_2 remain equal, we conclude that f_{τ_1, τ_2} . Now it follows that $(1 + z_{\tau_1+1})^{\tau_1+1} = (1 + z_{\tau_1})^{\tau_1} (1 + f_{\tau_1, \tau_2})$ and $(1 + z_{\tau_1+2})^{\tau_1+2} = (1 + z_{\tau_1})^{\tau_1} (1 + f_{\tau_1, \tau_2})^2$, etc. This allows us to rewrite (42) to

$$(1 + z_{\tau_1})^{\tau_1} (1 + f_{\tau_1, \tau_2})^{\tau_2 - \tau_1} = \left(\frac{1 + r_{\tau_2}}{1 - \sum_{t=1}^{\tau_1} \frac{r_{\tau_2}}{(1+z_t)^t} - \sum_{j=1}^{\tau_2 - \tau_1 - 1} \frac{r_{\tau_2}}{(1+z_{\tau_1})^{\tau_1} (1+f)^j}} \right)^{\tau_2}. \quad (45)$$

This allows us to calculate $1 + f_{\tau_1, \tau_2}$ numerically by solving

$$(1 + z_{\tau_1})^{\tau_1} (1 + f_{\tau_1, \tau_2})^{\tau_2 - \tau_1} - \left(\frac{1 + r_{\tau_2}}{1 - \sum_{t=1}^{\tau_1} \frac{r_{\tau_2}}{(1+z_t)^t} - \sum_{j=1}^{\tau_2 - \tau_1 - 1} \frac{r_{\tau_2}}{(1+z_{\tau_1})^{\tau_1} (1+f)^j}} \right)^{\tau_2} = 0 \quad (46)$$

for f_{τ_1, τ_2} , which allows us to calculate z_t for $\tau_1 < t \leq \tau_2$, since we can rewrite (44) to $(1 + z_t)^t = (1 + z_{\tau_1})^{\tau_1} (1 + f_{\tau_1, \tau_2})^{t - \tau_1}$.

B Calculation $A(\tau)$ and $B(\tau)$

This appendix shows the analytical solutions to $A(\tau)$ and $B(\tau)$. The derivation of these solutions are given in Muns (2015).

$$A(\tau) = a_0 + a_0^{(1)}\tau + \sum_{i=1}^k \left\{ a_i \exp(-\lambda_i\tau) + \sum_{j=1}^k a_{ij} \exp(-(\lambda_i + \lambda_j)\tau) \right\} \quad (47)$$

$$a_0 = \sum_{i=1}^k \left\{ \frac{a_i^{(1)}}{\lambda_i} + \sum_{j=1}^k \frac{a_{ij}^{(1)}}{\lambda_i + \lambda_j} \right\} \quad a_i = -\frac{a_i^{(1)}}{\lambda_i} \quad a_{ij} = -\frac{a_{ij}^{(1)}}{\lambda_i + \lambda_j} \quad (48)$$

$$a_0^{(1)} = \left(\frac{1}{2}b_0 - \tilde{\Lambda}_0 \right)' b_0 - \delta_{0R} \quad a_i^{(1)} = (b_0 - \tilde{\Lambda}_0)' b_i \quad a_{ij} = \frac{1}{2}b_i' b_j \quad (49)$$

$$b_i = \frac{1}{\lambda_i} (v_i v_i^{-1}) \delta_{1R}, \quad i = 1, \dots, k \quad (50)$$

$$M = V_\lambda D_\lambda V_\lambda^{-1} \quad V_\lambda = [v_1, \dots, v_k] \quad V_\lambda^{-1} = [v_1^{-1}, \dots, v_k^{-1}]', \quad (51)$$

where $M = (\tilde{\Lambda}_1 + K)'$.

$$B(\tau) = b_0 + \sum_{i=1}^k b_i \exp(-\lambda_i\tau) \quad (52)$$

C Vector Ornstein-Uhlenbeck process

This appendix is following the approach from Appendix A of Pelsser (2019).

Starting with a system of linear ordinary differential equations (ODE's):

$$\frac{dy(t)}{dt} = Ay(t), \quad (53)$$

where $y(0) = y_0$ can be a vector of any length. Then (53) can be rewritten as

$$y(t) = \exp(At)y_0. \quad (54)$$

In the case that A can be diagonalised, we can rewrite

$$\exp(At) = V \exp(Dt) V^{-1}, \quad (55)$$

where $A = VDV^{-1}$, where D is diagonal and V contains the eigenvectors of A . Now we can differentiate with respect to t , leading to

$$\frac{d \exp(At)}{dt} = \sum_{n=1}^{\infty} \frac{A^n n t^{n-1}}{n!} = \exp(At)A. \quad (56)$$

This confirms that (54) holds as a solution for (53).

Now we consider the vector-OU process

$$dY_t = (a + AY_t)dt + CdW_t, \quad (57)$$

where Y_t is a d -dimensional stochastic process, a is a constant d -dimensional vector, A is a constant $d \times d$ -dimensional matrix, W_t is a k -dimensional Brownian Motion, and C is a constant $d \times k$ -dimensional matrix. We can use process $\exp(-At)Y_t$ and Itô's lemma to derive the answer for (53), leading us to

$$\begin{aligned} d \exp(-At)Y_t &= (-A \exp(-At)Y_t + \exp(-At)(a + AY_t)dt + \exp(-At)CdW_t \\ &= \exp(-At)adt + \exp(-At)CdW_t \end{aligned} \quad (58)$$

Then for $T > t$ the solution of (58) is given by

$$Y_T = \exp(A(T-t))Y_t + \int_t^T \exp(A(T-u))adu + \int_t^T \exp(A(T-u))CdW_u. \quad (59)$$

This allows us to derive the conditional distribution:

$$f(Y_T|Y_t) \sim N \left(\exp(A(T-t))Y_t + \int_t^T \exp(A(T-u))adu; \int_t^T \exp(A(T-u))CC' \exp(A'(T-u))du \right) \quad (60)$$

The terms containing matrix exponentials can be calculated, using the fact that these terms solve the following ODE's:

$$\frac{d \int_0^\tau \exp(A(T-u))adu}{dt} = a + A \left(\int_0^\tau \exp(A(T-u))adu \right), \quad (61)$$

$$\begin{aligned} \frac{d \exp(A(T-u))CC' \exp(A'(T-u))du}{dt} &= A \exp(A(T-u))CC' \exp(A'(T-u))du + \\ &\exp(A(T-u))CC' \exp(A'(T-u))duA' + CC', \end{aligned} \quad (62)$$

where both equations have initial conditions equal to zero in the vector and matrix form respectively, since in that case the integral goes from zero to zero. The model is time-homogenous i.e., the parameters do not change over time, thus we can define $\tau := T - t$ to simplify our notation. However, for small Δt we can use Euler discretization to approximate the vector-OU process:

$$Y_{t+\Delta t} - Y_t = (a + AY_t)\Delta t + C(W_{t+\Delta t} - W_t) + O(\Delta t^{3/2}). \quad (63)$$

The discretization allows us to bypass the calculation of the matrix exponentials, after which we can approximate the conditional distribution for small Δt :

$$f(Y_{t+\Delta t}|Y_t) \approx N((I + A\Delta t)Y_t + a\Delta t; CC'\Delta t). \quad (64)$$

D Estimated parameters

	Diffuse prior	Stationary prior
$\delta_{0\pi}$	1.2539	1.2501
$\delta_{1\pi,1}$	0.0722	0.0677
$\delta_{1\pi,2}$	-0.0394	-0.0394
δ_{0r}	3.6602	3.2077
$\delta_{1r,1}$	1.8781	1.8867
$\delta_{1r,2}$	-1.5663	-1.5318
K_{11}	-0.6857	-0.6220
K_{22}	-0.5912	-0.4110
K_{21}	106.6488	105.7645
$\sigma_{\Pi,1}$	-0.0425	-0.0464
$\sigma_{\Pi,2}$	-0.3007	-0.3050
$\sigma_{\Pi,3}$	-1.7162	-1.7159
η_S	-7.4642	-7.0942
$\sigma_{S,1}$	5.6150	4.9107
$\sigma_{S,2}$	-14.9331	-13.9527
$\sigma_{S,3}$	-2.7143	-2.6387
$\sigma_{S,4}$	49.1346	49.1187
$\lambda_{0,1}$	-1576.5478	-1523.3475
$\lambda_{0,2}$	758.6516	755.0843
$\tilde{\Lambda}_{1,1}$	148.3994	148.4292
$\tilde{\Lambda}_{1,2}$	32.4658	30.6260
$\tilde{\Lambda}_{2,1}$	-212.2957	-216.0061
$\tilde{\Lambda}_{2,2}$	-15.9361	-15.7957
h_1	0.0271	0.0275
h_5	0.0023	0.0022
h_{10}	0.0000	0.0000
h_{15}	0.0002	0.0002
h_{20}	0.0000	0.0000
h_{30}	0.0016	0.0016
Full sample log-likelihood	12067.44	12026.41
Log-likelihood until October 2008	5287.70	5246.77
Log-likelihood after October 2008	6779.74	6779.64

Table 4: Estimated parameters ($\times 1000$) and corresponding log-likelihoods of the two-factor model.

	Until break	After break
$\delta_{0\pi}$	1.9113	1.0152
$\delta_{1\pi,1}$	0.0373	0.0536
$\delta_{1\pi,2}$	0.0287	-0.0540
δ_{0r}	5.9058	0.0001
$\delta_{1r,1}$	2.7209	1.3450
$\delta_{1r,2}$	-0.8947	-1.3954
K_{11}	0.8516	-1.0470
K_{22}	15.1874	-0.9906
K_{21}	10.0704	39.0191
$\sigma_{\Pi,1}$	-0.1449	0.0646
$\sigma_{\Pi,2}$	-0.2674	-0.4083
$\sigma_{\Pi,3}$	-1.5166	-1.8704
η_S	-22.3995	-0.4706
$\sigma_{S,1}$	11.6639	-2.3787
$\sigma_{S,2}$	-2.4476	-11.0784
$\sigma_{S,3}$	7.3431	-5.1614
$\sigma_{S,4}$	45.3995	47.6475
$\lambda_{0,1}$	-2165.2574	-1107.9313
$\lambda_{0,2}$	713.6128	787.4767
$\tilde{\Lambda}_{1,1}$	154.3587	158.1741
$\tilde{\Lambda}_{1,2}$	69.3955	61.5816
$\tilde{\Lambda}_{2,1}$	-74.4276	-189.3830
$\tilde{\Lambda}_{2,2}$	-24.7130	-34.3365
h_1	0.0257	0.0317
h_5	0.0015	0.0023
h_{10}	0.0000	0.0000
h_{15}	0.0000	0.0002
h_{20}	0.0000	0.0000
h_{30}	0.0002	0.0012
Full sample log-likelihood	8495.30	11610.24
Log-likelihood until October 2008	5499.19	4629.47
Log-likelihood after October 2008	2996.11	6980.77

Table 5: Estimated parameters ($\times 1000$) and corresponding log-likelihoods in the two-factor model before and after the break with a diffuse prior.

	Until break	After break
$\delta_{0\pi}$	2.3563	1.0768
$\delta_{1\pi,1}$	0.0180	0.0460
$\delta_{1\pi,2}$	0.0432	-0.0487
δ_{0r}	2.0089	0.0001
$\delta_{1r,1}$	2.5468	1.3893
$\delta_{1r,2}$	-1.3265	-1.3581
K_{11}	4.4181	99.2483
K_{22}	13.3004	17.1775
K_{21}	26.6669	56.0048
$\sigma_{\Pi,1}$	-0.1911	0.0517
$\sigma_{\Pi,2}$	-0.2777	-0.4007
$\sigma_{\Pi,3}$	-1.5239	-1.8682
η_S	-30.6398	0.6198
$\sigma_{S,1}$	12.6222	-8.2539
$\sigma_{S,2}$	-3.7230	-8.6708
$\sigma_{S,3}$	9.0745	-5.1874
$\sigma_{S,4}$	44.4302	47.5254
$\lambda_{0,1}$	-1709.7635	-1794.5365
$\lambda_{0,2}$	982.4166	1395.9101
$\tilde{\Lambda}_{1,1}$	149.0715	62.5941
$\tilde{\Lambda}_{1,2}$	40.6089	65.5438
$\tilde{\Lambda}_{2,1}$	-119.6867	-211.9599
$\tilde{\Lambda}_{2,2}$	-17.4417	-57.5418
h_1	0.0244	0.0324
h_5	0.0014	0.0025
h_{10}	0.0000	0.0000
h_{15}	0.0000	0.0002
h_{20}	0.0000	0.0000
h_{30}	0.0002	0.0013
Full sample log-likelihood	7915.74	11616.82
Log-likelihood until October 2008	5458.74	4638.44
Log-likelihood after October 2008	2457.00	6978.38

Table 6: Estimated parameters ($\times 1000$) and corresponding log-likelihoods in the two-factor model before and after the break with a stationary prior.

	Diffuse prior	Stationary prior		Diffuse prior	Stationary prior
$\delta_{0\pi}$	1.8984	1.8982	$\lambda_{0,1}$	341.1780	341.1756
$\delta_{1\pi,1}$	-1.2876	-1.3581	$\lambda_{0,2}$	3050.0168	3050.0155
$\delta_{1\pi,2}$	2.4179	2.5549	$\lambda_{0,3}$	2455.9721	2455.9751
$\delta_{1\pi,3}$	-0.0190	-0.0203	$\tilde{\Lambda}_{1,1}$	-184.0783	-184.0368
δ_{0r}	43.6805	43.6900	$\tilde{\Lambda}_{1,2}$	-22.6596	-22.6363
$\delta_{1r,1}$	-0.2490	-0.2343	$\tilde{\Lambda}_{2,1}$	-633.1985	-633.1824
$\delta_{1r,2}$	-0.0808	-0.0823	$\tilde{\Lambda}_{2,2}$	-1439.5350	-1439.5223
$\delta_{1r,3}$	-1.7549	-1.7686	$\tilde{\Lambda}_{1,3}$	289.1358	289.1664
K_{11}	0.1998	0.1318	$\tilde{\Lambda}_{2,3}$	1544.2839	1544.2976
K_{22}	1964.3792	1964.3181	$\tilde{\Lambda}_{3,1}$	-315.8296	-315.8594
K_{21}	-1020.4152	-1020.2809	$\tilde{\Lambda}_{3,2}$	-1258.2063	-1258.2215
K_{31}	-763.6775	-763.5055	$\tilde{\Lambda}_{3,3}$	1197.4008	1197.3701
K_{32}	1469.7013	1469.5991	h_1	0.0000	0.0000
K_{33}	-0.7619	-0.7457	h_5	0.0022	0.0022
$\sigma_{\Pi,1}$	0.1627	0.2062	h_{10}	0.0004	0.0004
$\sigma_{\Pi,2}$	0.1273	0.0858	h_{15}	0.0000	0.0000
$\sigma_{\Pi,3}$	0.5760	0.5885	h_{20}	0.0004	0.0004
$\sigma_{\Pi,4}$	1.1564	1.1348	h_{30}	0.0046	0.0046
η_S	-10.3358	-10.3275	Full sample $\ln(L)$	12166.64	12129.34
$\sigma_{S,1}$	-9.7307	-9.7401	$\ln(L)$ until October 2008	5302.95	5264.75
$\sigma_{S,2}$	25.5630	25.5631	$\ln(L)$ after October 2008	6865.95	6864.44
$\sigma_{S,3}$	6.9173	6.9123			
$\sigma_{S,4}$	-21.9699	-21.9727			
$\sigma_{S,5}$	35.9459	35.9470			

Table 7: Estimated parameters ($\times 1000$) and corresponding log-likelihoods of the three-factor model.

	Until break	After break		Until break	After break
$\delta_{0\pi}$	2.9484	1.7674	$\lambda_{0,1}$	1229.7383	-85.4479
$\delta_{1\pi,1}$	-0.4321	-1.2895	$\lambda_{0,2}$	2326.7648	3855.3947
$\delta_{1\pi,2}$	0.8790	2.3403	$\lambda_{0,3}$	3523.9271	2489.8825
$\delta_{1\pi,3}$	-0.0547	0.0194	$\tilde{\Lambda}_{1,1}$	-464.1745	-307.8430
δ_{0r}	21.3453	26.2292	$\tilde{\Lambda}_{1,2}$	330.1380	-26.5482
$\delta_{1r,1}$	-0.0802	-0.9329	$\tilde{\Lambda}_{2,1}$	-325.8254	-730.4128
$\delta_{1r,2}$	-0.9937	0.4207	$\tilde{\Lambda}_{2,2}$	-288.2055	-1085.0208
$\delta_{1r,3}$	-2.8202	-1.2743	$\tilde{\Lambda}_{1,3}$	622.2274	470.1695
K_{11}	8.4532	0.3382	$\tilde{\Lambda}_{2,3}$	971.1863	1776.9632
K_{22}	1075.8936	1727.3385	$\tilde{\Lambda}_{3,1}$	-634.6868	-446.3443
K_{21}	-571.0551	-912.1682	$\tilde{\Lambda}_{3,2}$	-105.7352	-1262.5367
K_{31}	-601.5277	-834.6769	$\tilde{\Lambda}_{3,3}$	1403.3460	1511.1807
K_{32}	1135.2567	1584.5133	h_1	0.0000	0.0000
K_{33}	8.9335	-0.0096	h_5	0.0017	0.0021
$\sigma_{\Pi,1}$	0.0536	0.0008	h_{10}	0.0003	0.0003
$\sigma_{\Pi,2}$	-0.9334	0.3563	h_{15}	0.0000	0.0000
$\sigma_{\Pi,3}$	0.1783	0.6351	h_{20}	0.0002	0.0003
$\sigma_{\Pi,4}$	1.2556	1.0415	h_{30}	0.0011	0.0026
η_S	31.1507	-7.3774	Full sample $\ln(L)$	10850.01	10438.84
$\sigma_{S,1}$	-13.7476	-16.8398	$\ln(L)$ until October 2008	5439.67	3359.42
$\sigma_{S,2}$	10.5060	29.9903	$\ln(L)$ after October 2008	5412.34	7076.99
$\sigma_{S,3}$	-13.1846	13.1617			
$\sigma_{S,4}$	2.1297	-29.2077			
$\sigma_{S,5}$	47.6948	3.8907			

Table 8: Estimated parameters ($\times 1000$) and corresponding log-likelihoods in the three-factor model before and after the break with a diffuse prior.

	Until break	After break		Until break	After break
$\delta_{0\pi}$	1.0124	1.0744	$\lambda_{0,1}$	764.0047	107.3769
$\delta_{1\pi,1}$	-0.0038	-1.2442	$\lambda_{0,2}$	1185.0668	3276.8223
$\delta_{1\pi,2}$	0.0402	2.0563	$\lambda_{0,3}$	1920.0769	1927.6871
$\delta_{1\pi,3}$	-0.0348	-0.0119	$\tilde{\Lambda}_{1,1}$	-670.4909	-252.0732
δ_{0r}	56.8349	3.9251	$\tilde{\Lambda}_{1,2}$	671.9924	-39.5558
$\delta_{1r,1}$	0.3359	-0.2885	$\tilde{\Lambda}_{2,1}$	-231.0403	-951.9042
$\delta_{1r,2}$	-1.5200	0.3565	$\tilde{\Lambda}_{2,2}$	-42.9496	-949.4717
$\delta_{1r,3}$	-2.6151	-1.3624	$\tilde{\Lambda}_{1,3}$	575.1340	258.8472
K_{11}	0.2580	25.6164	$\tilde{\Lambda}_{2,3}$	646.6484	2075.6138
K_{22}	1143.0140	1528.7990	$\tilde{\Lambda}_{3,1}$	-1069.9041	-644.0185
K_{21}	-743.7412	-891.1117	$\tilde{\Lambda}_{3,2}$	1001.9533	-1177.5787
K_{31}	-303.8618	-772.2684	$\tilde{\Lambda}_{3,3}$	986.1762	1547.4083
K_{32}	468.3076	1375.2360	h_1	0.0000	0.0000
K_{33}	3.5396	-1.8104	h_5	0.0008	0.0017
$\sigma_{\Pi,1}$	-0.1383	0.1516	h_{10}	0.0001	0.0003
$\sigma_{\Pi,2}$	-0.2351	0.2219	h_{15}	0.0000	0.0000
$\sigma_{\Pi,3}$	0.2506	0.5438	h_{20}	0.0001	0.0002
$\sigma_{\Pi,4}$	1.4304	1.1996	h_{30}	0.0004	0.0016
η_S	-16.5922	17.3588	Full sample $\ln(L)$	9171.67	9490.11
$\sigma_{S,1}$	-8.7509	-11.7820	$\ln(L)$ until October 2008	5535.09	2370.57
$\sigma_{S,2}$	9.2091	35.2618	$\ln(L)$ after October 2008	3618.49	7118.06
$\sigma_{S,3}$	-21.8969	13.5242			
$\sigma_{S,4}$	-4.1092	-23.6864			
$\sigma_{S,5}$	43.8769	10.4715			

Table 9: Estimated parameters ($\times 1000$) and corresponding log-likelihoods in the three-factor model before and after the break with a stationary prior.

E Bootstrapped Histograms

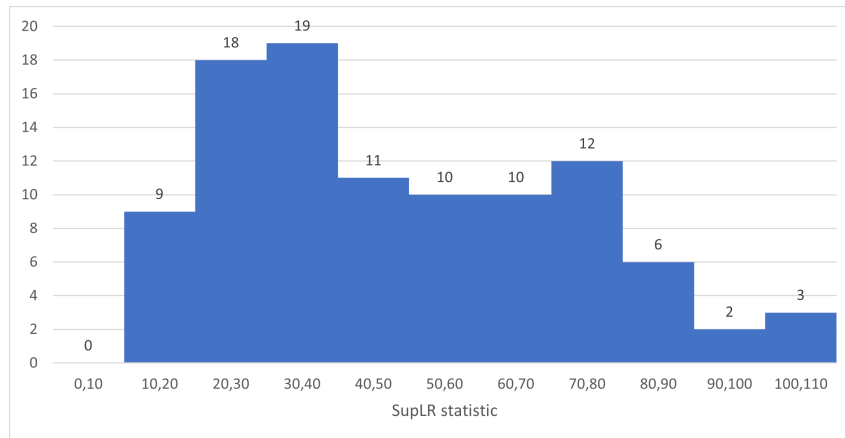


Figure 8: Histogram of bootstrapped SupLR statistics in the two-factor model with diffuse prior.

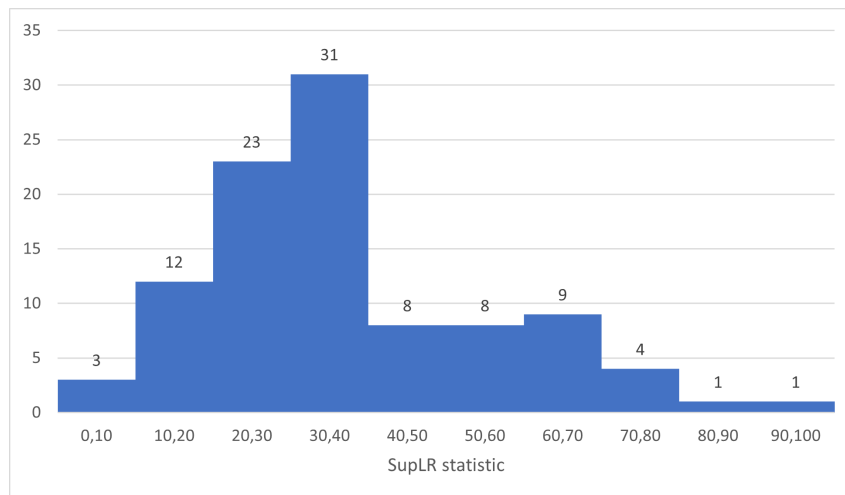


Figure 9: Histogram of bootstrapped SupLR statistics in the two-factor model with stationary prior.

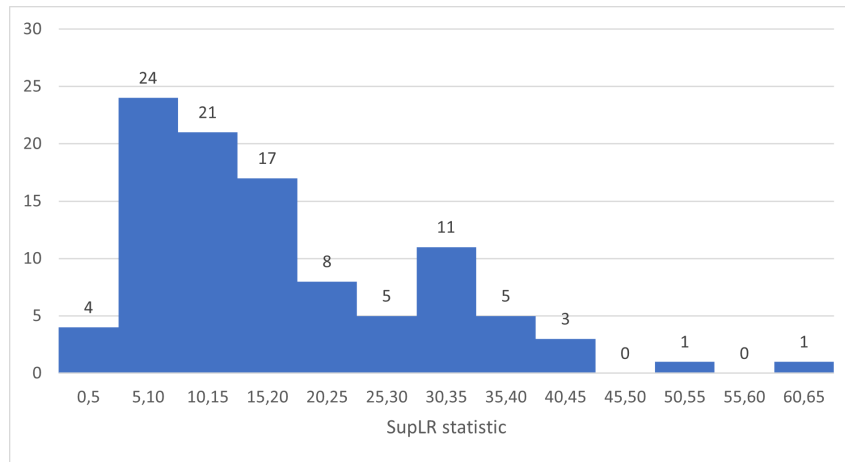


Figure 10: Histogram of bootstrapped SupLR statistics in the three-factor model with diffuse prior.

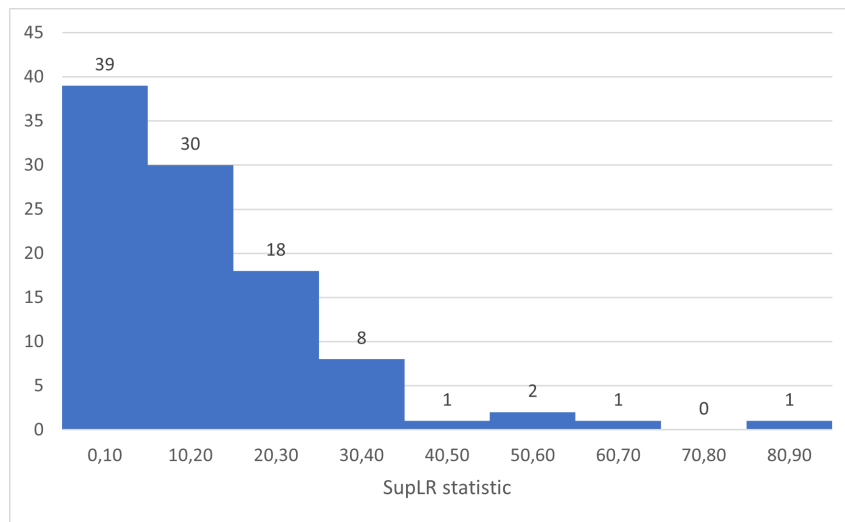


Figure 11: Histogram of bootstrapped SupLR statistics in the three-factor model with stationary prior.

F Descriptive statistics before and after October 2008

	Mean	Standard deviation
$\Delta \ln(\text{Price Index})$	1.860	1.562
$\Delta \ln(\text{Stock Index})$	-1.253	45.301
$\Delta y_t(1)$	0.146	1.876
$\Delta y_t(5)$	0.081	2.197
$\Delta y_t(10)$	0.021	1.854
$\Delta y_t(15)$	-0.011	1.741
$\Delta y_t(20)$	-0.041	1.677
$\Delta y_t(30)$	-0.084	1.646

Table 10: Summary statistics of the first-differenced series ($\times 1000$) until October 2008.

	Mean	Standard deviation
$\Delta \ln(\text{Price Index})$	0.988	1.562
$\Delta \ln(\text{Stock Index})$	7.839	45.301
$\Delta y_t(1)$	-0.301	1.162
$\Delta y_t(5)$	-0.284	1.523
$\Delta y_t(10)$	-0.289	1.780
$\Delta y_t(15)$	-0.281	1.966
$\Delta y_t(20)$	-0.263	2.036
$\Delta y_t(30)$	-0.233	2.067

Table 11: Summary statistics of the first-differenced series ($\times 1000$) after October 2008.

G Eigenvalues of Φ

Diffuse prior	Stationary prior	Until break (D)	After break (D)	Until break (S)	After break (S)
1	1	1	1	1	1
1	1	1	1	1	1
1.001*	1.000*	0.985	1.001*	0.987	0.983
1.001*	1.001*	0.999	1.001*	0.996	0.906

Table 12: Eigenvalues of Φ in the two-factor model. (S): Stationary prior, (D): Diffuse prior, *: eigenvalue exceeds 1.

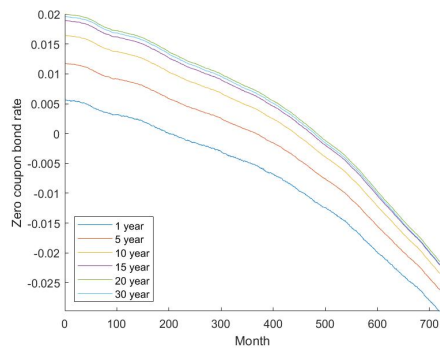
Diffuse prior	Stationary prior	Until break (D)	After break (D)	Until break (S)	After break (S)
1	1	1	1	1	1
1	1	1	1	1	1
1.001*	1.001*	0.991	1.000*	0.996	1.002*
0.140	0.140	0.341	0.178	0.319	0.217
1.000	1.000	0.992	1.000	1.000	0.975

Table 13: Eigenvalues of Φ in the three-factor model. (S): Stationary prior, (D): Diffuse prior, *: eigenvalue exceeds 1.

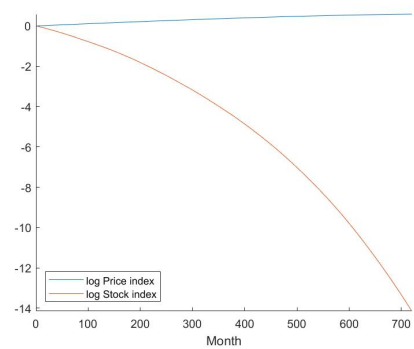
Diffuse prior	Stationary prior	DNB parameters
1	1	1
1	1	1
0.296	0.298	0.299
1.076	0.961	0.953

Table 14: Eigenvalues of Φ from Pelsser (2019). (*) : eigenvalue exceeds 1

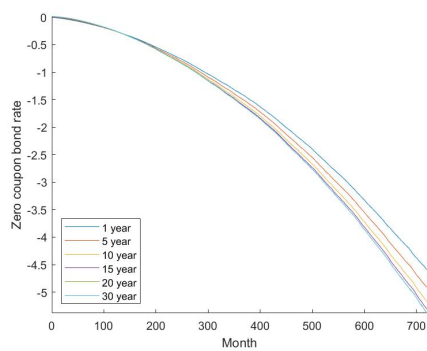
H Individual mean and 5th percentile of simulated scenarios



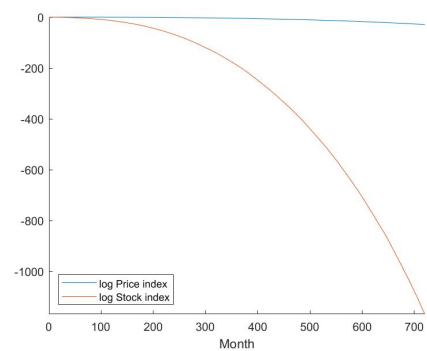
(a) Mean of ZCB rates



(b) Mean of log price and stock indices

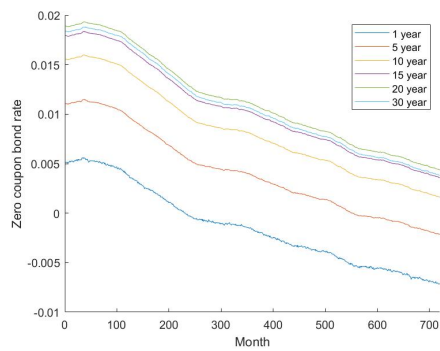


(c) 5th percentile of ZCB rates

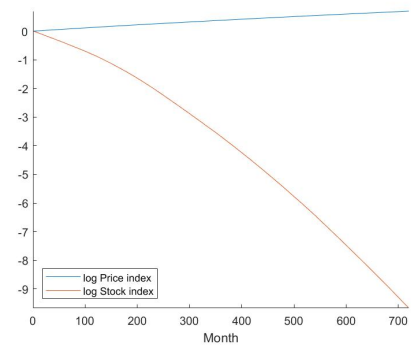


(d) 5th percentile of log price and stock indices

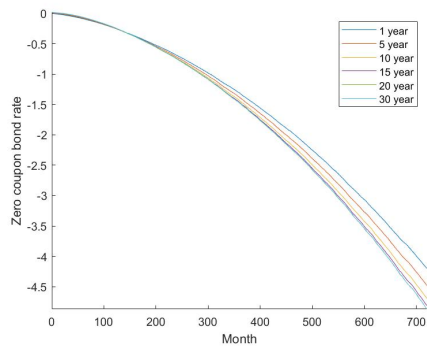
Figure 12: Two-factor diffuse case



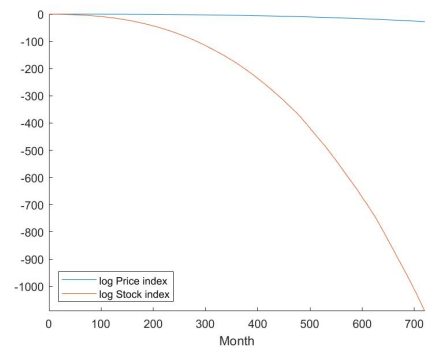
(a) Mean of ZCB rates



(b) Mean of log price and stock indices

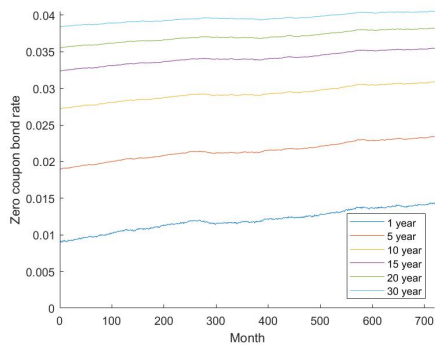


(c) 5th percentile of ZCB rates

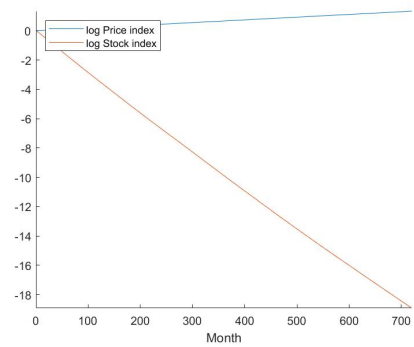


(d) 5th percentile of log price and stock indices

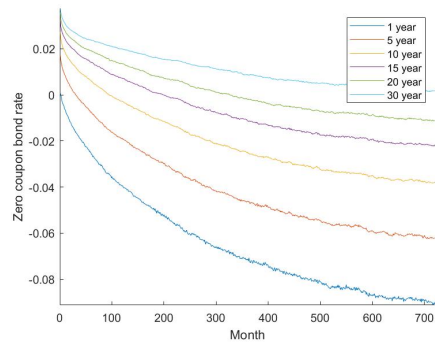
Figure 13: Two-factor stationary case



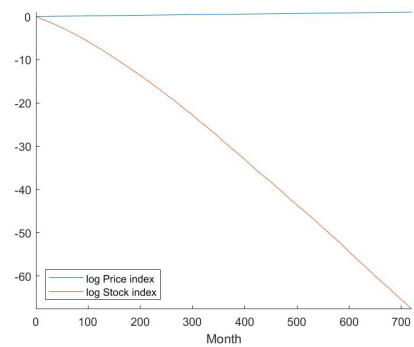
(a) Mean of ZCB rates



(b) Mean of log price and stock indices

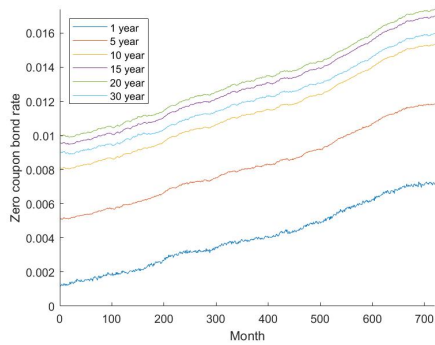


(c) 5th percentile of ZCB rates

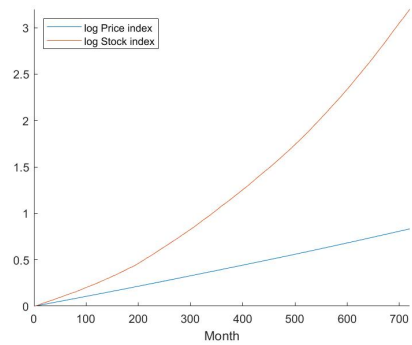


(d) 5th percentile of log price and stock indices

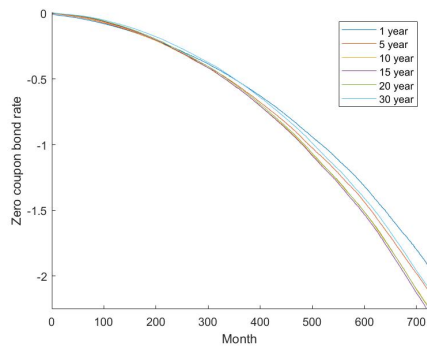
Figure 14: Two-factor diffuse case prior to the first break



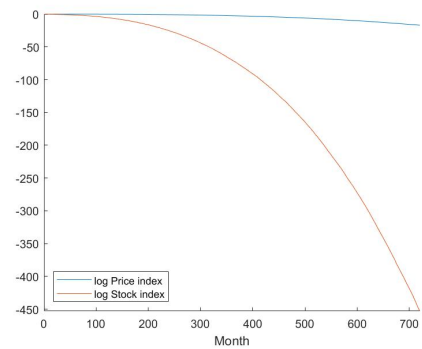
(a) Mean of ZCB rates



(b) Mean of log price and stock indices

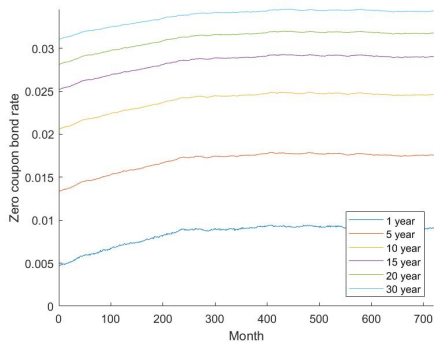


(c) 5th percentile of ZCB rates

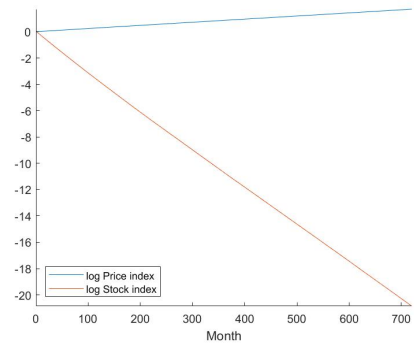


(d) 5th percentile of log price and stock indices

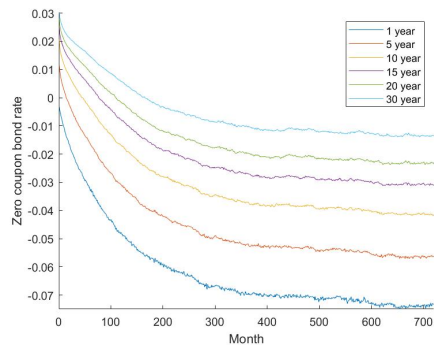
Figure 15: Two-factor diffuse case after the first break



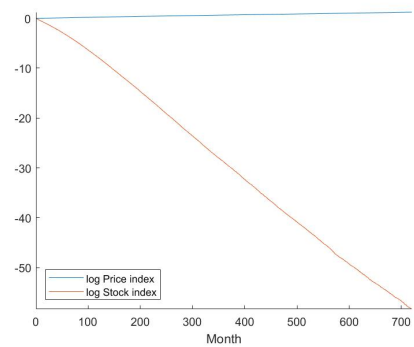
(a) Mean of ZCB rates



(b) Mean of log price and stock indices

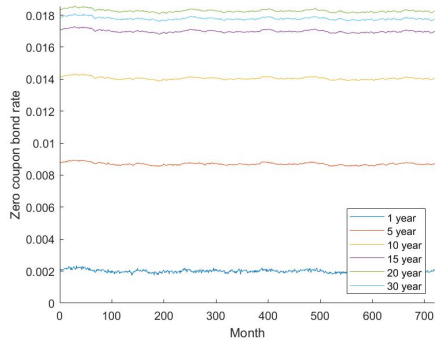


(c) 5th percentile of ZCB rates

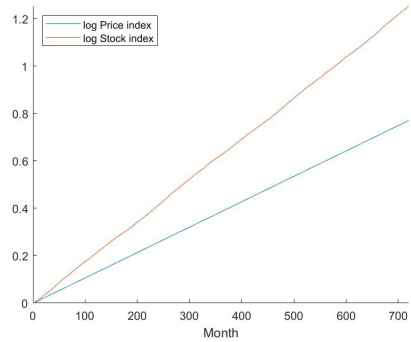


(d) 5th percentile of log price and stock indices

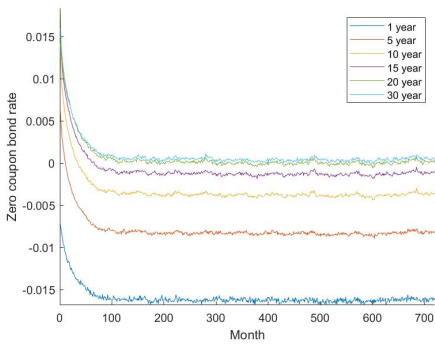
Figure 16: Two-factor stationary case prior to the first break



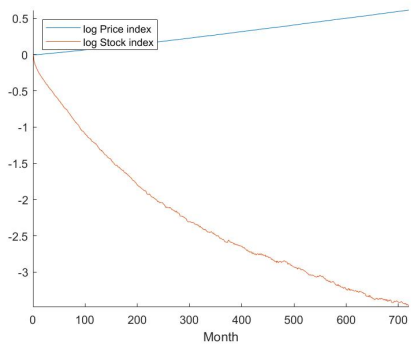
(a) Mean of ZCB rates



(b) Mean of log price and stock indices

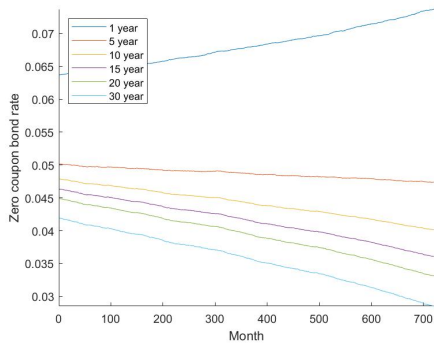


(c) 5th percentile of ZCB rates

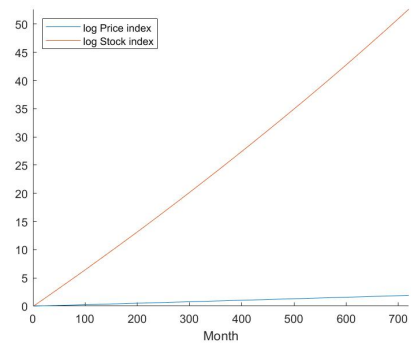


(d) 5th percentile of log price and stock indices

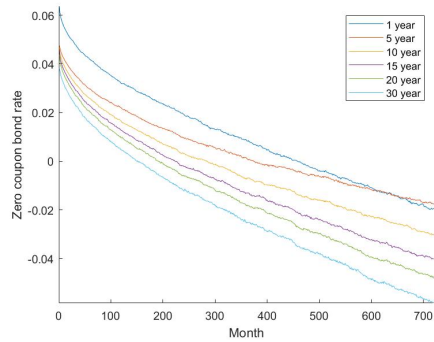
Figure 17: Two-factor stationary case after the first break



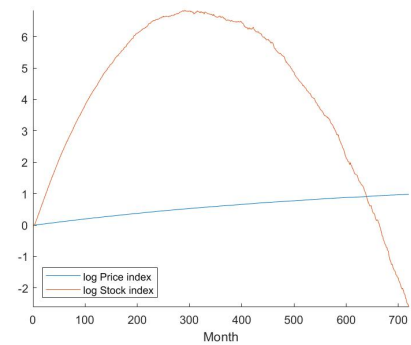
(a) Mean of ZCB rates



(b) Mean of log price and stock indices

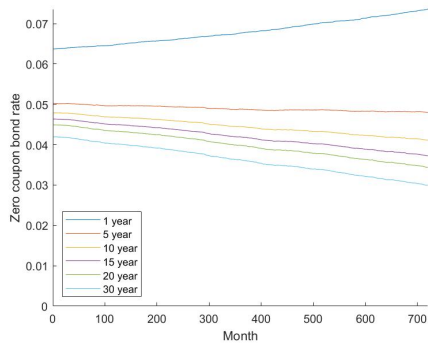


(c) 5th percentile of ZCB rates

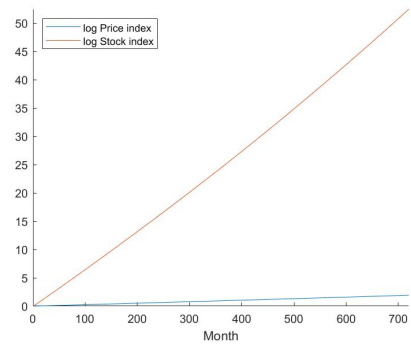


(d) 5th percentile of log price and stock indices

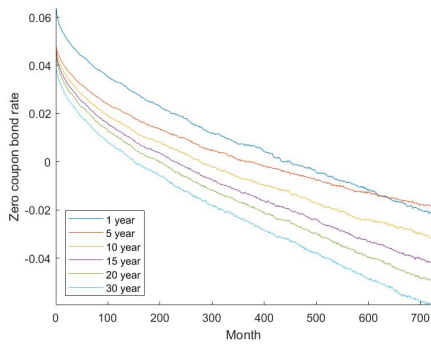
Figure 18: Three-factor diffuse case



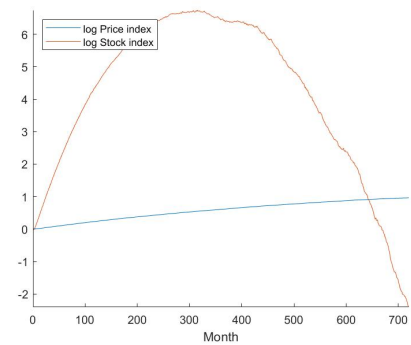
(a) Mean of ZCB rates



(b) Mean of log price and stock indices

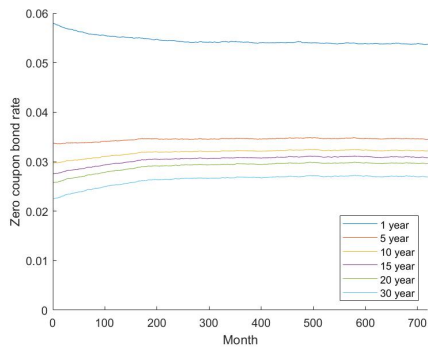


(c) 5th percentile of ZCB rates

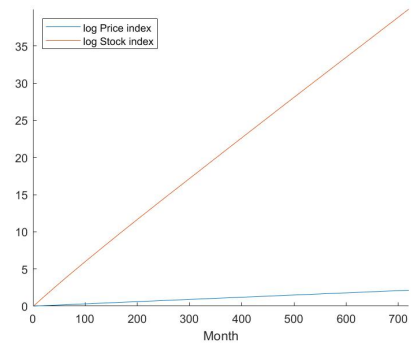


(d) 5th percentile of log price and stock indices

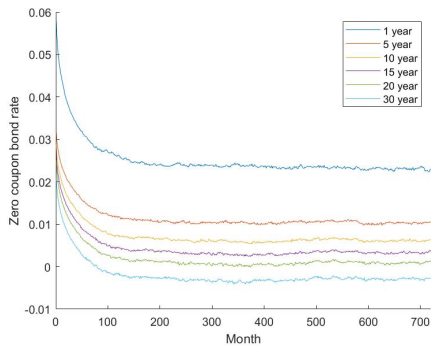
Figure 19: Three-factor stationary case



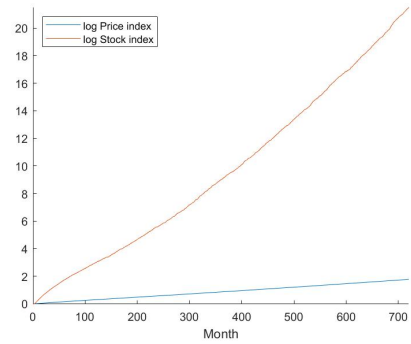
(a) Mean of ZCB rates



(b) Mean of log price and stock indices

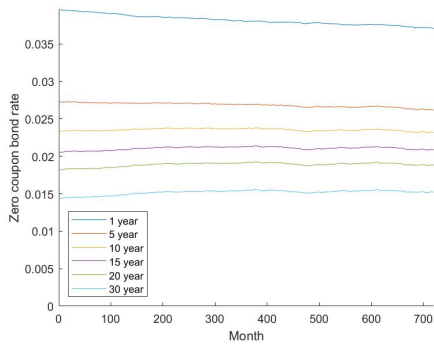


(c) 5th percentile of ZCB rates

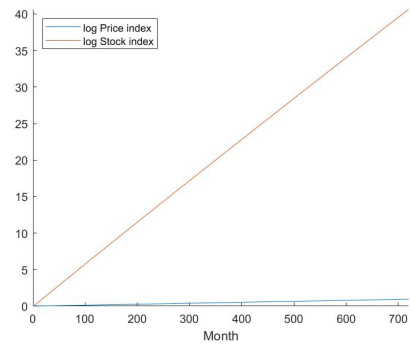


(d) 5th percentile of log price and stock indices

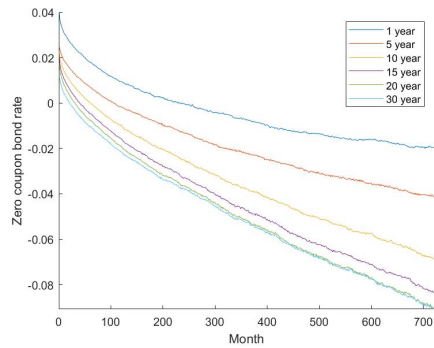
Figure 20: Three-factor diffuse case prior to the first break



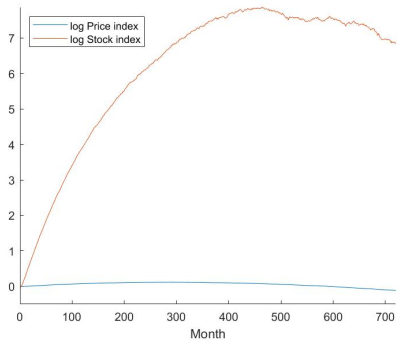
(a) Mean of ZCB rates



(b) Mean of log price and stock indices

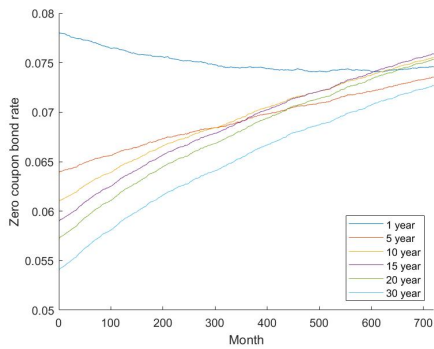


(c) 5th percentile of ZCB rates

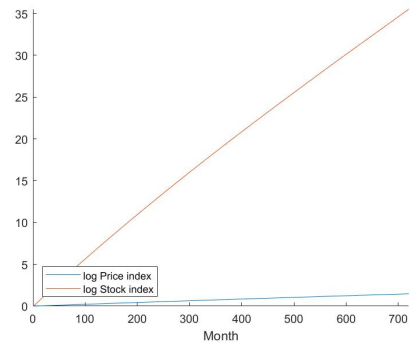


(d) 5th percentile of log price and stock indices

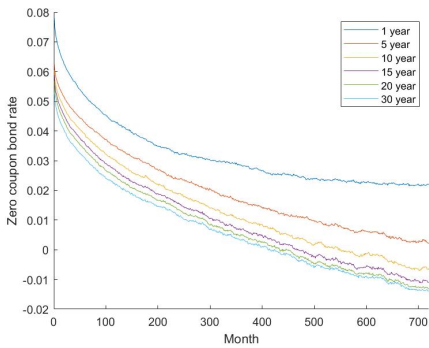
Figure 21: Three-factor diffuse case after the first break



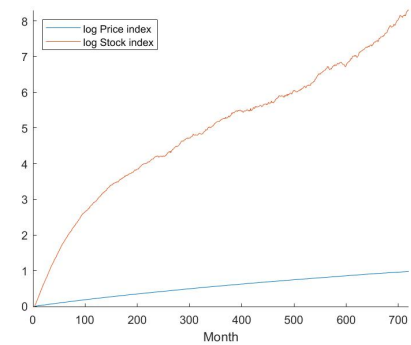
(a) Mean of ZCB rates



(b) Mean of log price and stock indices

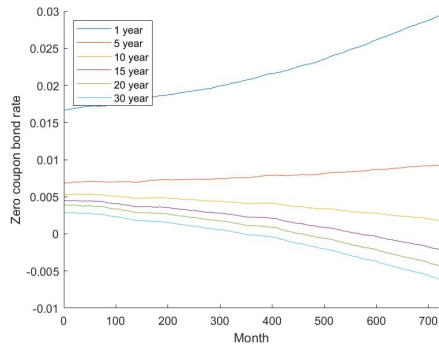


(c) 5th percentile of ZCB rates

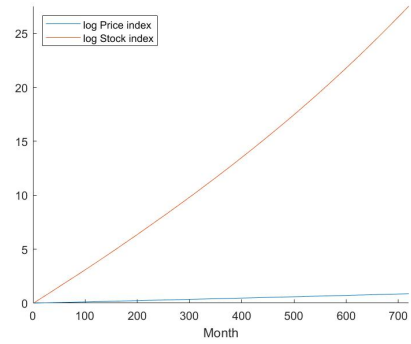


(d) 5th percentile of log price and stock indices

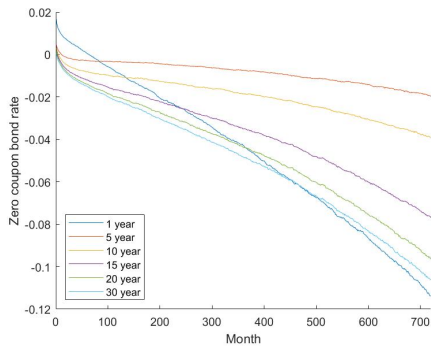
Figure 22: Three-factor stationary case prior to the first break



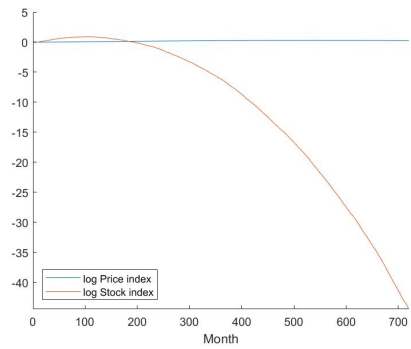
(a) Mean of ZCB rates



(b) Mean of log price and stock indices

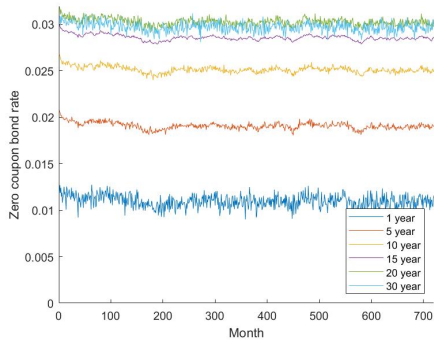


(c) 5th percentile of ZCB rates

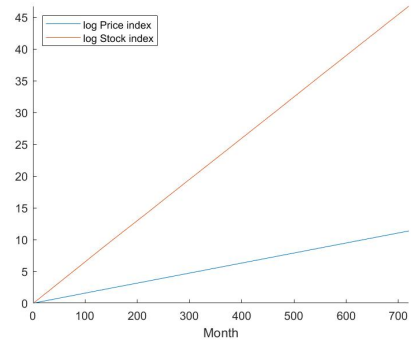


(d) 5th percentile of log price and stock indices

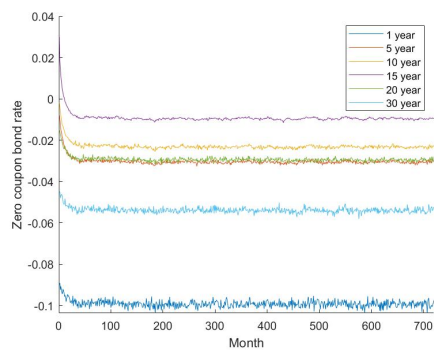
Figure 23: Three-factor stationary case after the first break



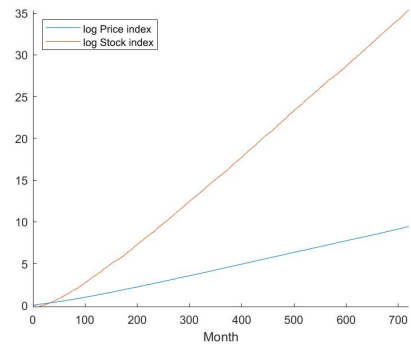
(a) Mean of ZCB rates



(b) Mean of log price and stock indices

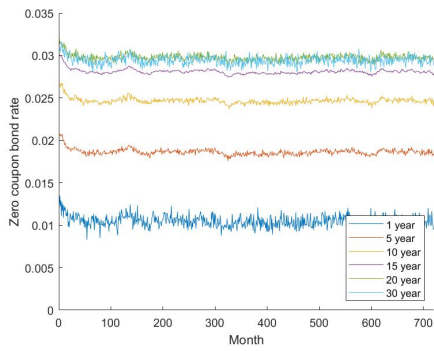


(c) 5th percentile of ZCB rates

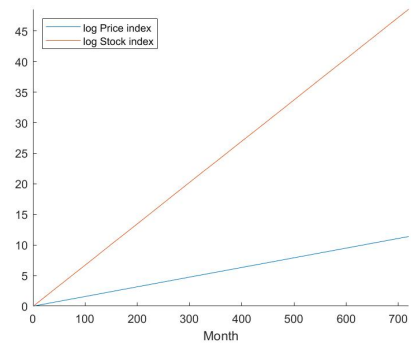


(d) 5th percentile of log price and stock indices

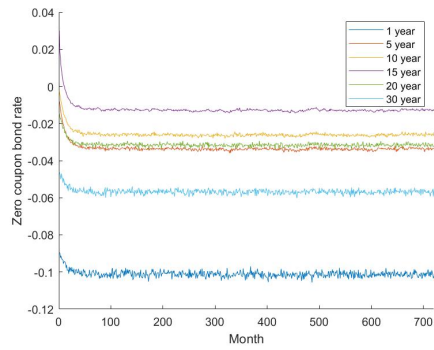
Figure 24: DNB parameters from Pelsser (2019)



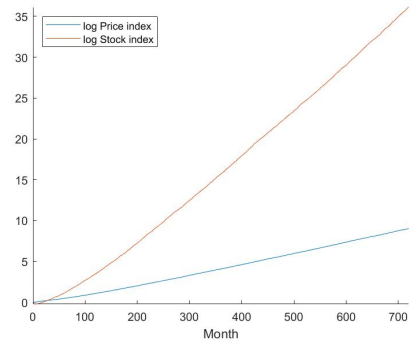
(a) Mean of ZCB rates



(b) Mean of log price and stock indices



(c) 5th percentile of ZCB rates



(d) 5th percentile of log price and stock indices

Figure 25: Stationary parameters from Pelsser (2019)

References

- Akaike, H. (1974). A new look at the statistical model identification. *IEEE transactions on automatic control*, 19(6):716–723.
- Andreasen, M., Jørgensen, K., and Meldrum, A. (2019). Bond risk premiums at the zero lower bound.
- Andrews, D. (1993). Tests for parameter instability and structural change with unknown change point. *Econometrica*, 61(4):821–56.
- Andrews, D. W. and Ploberger, W. (1994). Optimal tests when a nuisance parameter is present only under the alternative. *Econometrica*, pages 1383–1414.
- Bai, J. (1997). Estimating multiple breaks one at a time. *Econometric theory*, 13(3):315–352.
- Bai, J. and Perron, P. (1998). Estimating and testing linear models with multiple structural changes. *Econometrica*, pages 47–78.
- Bai, J. and Perron, P. (2003). Computation and analysis of multiple structural change models. *Journal of applied econometrics*, 18(1):1–22.
- Bouwman, K. E. and Lord, R. (2016). An overview of derivative pricing in gaussian affine asset pricing models: An application to the KNW model.
- Brennan, M. J. and Xia, Y. (2002). Dynamic asset allocation under inflation. *The Journal of Finance*, 57(3):1201–1238.
- Chong, T. T.-l. (1995). Partial parameter consistency in a misspecified structural change model. *Economics Letters*, 49(4):351–357.
- Cox, J. C., Ingersoll Jr, J. E., and Ross, S. A. (1985). An intertemporal general equilibrium model of asset prices. *Econometrica*, pages 363–384.
- Dai, Q. and Singleton, K. J. (2000). Specification analysis of affine term structure models. *The Journal of Finance*, 55(5):1943–1978.
- Delbaen, F. and Schachermayer, W. (1994). A general version of the fundamental theorem of asset pricing. *Mathematische annalen*, 300(1):463–520.
- Diebold, F. X. and Chen, C. (1996). Testing structural stability with endogenous breakpoint a size comparison of analytic and bootstrap procedures. *Journal of Econometrics*, 70(1):221–241.
- Dijsselbloem, J., De Waegenaere, A., van Ewijk, C., van der Horst, A., Knoef, M., and Steenbeek, O. (2019). Advies Commissie Parameters.
- Draper, N. (2014). A financial market model for The Netherlands. *CPB*.

- Duffee, G. R. (2002). Term premia and interest rate forecasts in affine models. *The Journal of Finance*, 57(1):405–443.
- Duffie, D. and Kan, R. (1996). A yield-factor model of interest rates. *Mathematical finance*, 6(4):379–406.
- European Central Bank (2021). Monetary policy decisions.
- Girsanov, I. V. (1960). On transforming a certain class of stochastic processes by absolutely continuous substitution of measures. *Theory of Probability & Its Applications*, 5(3):285–301.
- Hansen, P. R. (2003). Structural changes in the cointegrated vector autoregressive model. *Journal of Econometrics*, 114(2):261–295.
- Kim, D. H. (2007). Challenges in macro-finance modeling.
- Kim, D. H. and Wright, J. H. (2005). An arbitrage-free three-factor term structure model and the recent behavior of long-term yields and distant-horizon forward rates. Finance and Economics Discussion Series 2005-33, Board of Governors of the Federal Reserve System (U.S.).
- Koijen, R. S., Nijman, T. E., and Werker, B. J. (2010). When can life cycle investors benefit from time-varying bond risk premia? *The review of financial studies*, 23(2):741–780.
- Lemke, W. and Vladu, A. (2016). Below the zero lower bound: A shadow-rate term structure model for the euro area.
- Lever, M. (2019). Financieel toetsingskader (FTK). *Pensioenfederatie*.
- Litterman, R. and Scheinkman, J. (1991). Common factors affecting bond returns. *Journal of Fixed Income*, 1(1):54–61.
- Lütkepohl, H. (2005). *New introduction to multiple time series analysis*. Springer Science & Business Media.
- Marçal, E. F. and Pereira, P. L. V. (2014). Evaluating the existence of structural change in the brazilian term structure of interest rate: evidence based on hansens cointegration models with structural break. *São Paulo Journal of Mathematical Sciences*, 8(2):211–239.
- MATLAB Optimization Toolbox (2020). Matlab optimization toolbox. The MathWorks, Natick, MA, USA.
- Morley, J., Panovska, I., and Sinclair, T. M. (2011). A likelihood ratio test of stationarity based on a correlated unobserved components model. Technical report.
- Muns, S. (2015). A financial market model for the Netherlands: A methodological refinement.
- Pelsser, A. (2019). Kalman filter estimation of the KNW model.

- Schwarz, G. (1978). Estimating the dimension of a model. *The annals of statistics*, pages 461–464.
- Vasicek, O. (1977). An equilibrium characterization of the term structure. *Journal of Financial Economics*, 5(2):177–188.
- Wilks, S. S. (1938). The large-sample distribution of the likelihood ratio for testing composite hypotheses. *The annals of mathematical statistics*, 9(1):60–62.